

3D PHYSICS AND THE ELECTROWEAK PHASE TRANSITION: PERTURBATION THEORY

K. Farakos^{a1}, K. Kajantie^b, K. Rummukainen^c and M. Shaposhnikov^{d2}

^a*National Technical University of Athens, Physics Department,
Zografou Campus, GR 157 80, Athens, Greece*

^b*Department of Theoretical Physics, P.O.Box 9, 00014 University of Helsinki, Finland*

^c*Indiana University, Department of Physics, Swain Hall West 117, Bloomington IN
47405 USA*

^d*Theory Division, CERN,
CH-1211 Geneva 23, Switzerland*

Abstract

We develop a method for the construction of the effective potential at high temperatures based on the effective field theory approach and renormalization group. It allows one to sum up the leading logarithms in all orders of perturbation theory. The method reproduces the known one-loop and two-loop results in a very simple and economic way and clarifies the issue of the convergence of the perturbation theory. We also discuss the assumptions being made for the determination of the critical temperature of the electroweak phase transition, and analyse different perturbative uncertainties in its determination. These results are then used for the non-perturbative lattice Monte Carlo simulations of the EW phase transition in forthcoming paper.

CERN-TH.6973/94
IUHET-273
March 1994

¹Partially supported by a CEC Science program (SCI-CT91-0729).

²On leave of absence from Institute for Nuclear Research of Russian Academy of Sciences, Moscow 117312, Russia.

1 Introduction

The order of high temperature phase transitions in gauge theories [1] plays an important role in cosmology. For example, first order phase transitions in grand unified theories can drive an inflation [2]; a first order phase transition in the standard electroweak theory may be responsible for baryogenesis [3, 4].

As is well known, perturbation theory in gauge theories at high temperatures is intrinsically unreliable due to power-like infrared divergencies [5, 6]. In particular, the $g^6 T^4$ correction to the free energy, originating first on the 4-loop level, is in principle not computable by perturbative methods. These divergencies make the perturbative effective potential divergent at small ϕ . A logarithmic divergence appears at the 4-loop level and at higher loops one gets power singularities³. At non-zero ϕ the infrared problem is absent, since integrals at small momenta are cut by non-zero gauge boson masses.

In view of the above one expects that at sufficiently large ϕ perturbation theory is applicable. Therefore, perturbation theory seems to be quite suitable to answer the following question: "what is the derivative of the effective potential at *given* temperature and *sufficiently large* ϕ ?" Note that the absolute value of the potential does not have any physical meaning due to arbitrariness in the overall normalization (in the absence of gravitation). In particular, the expectation value of ϕ can be determined with the help of a perturbative effective potential provided that ϕ is large enough. However, the determination of the *critical temperature* of the phase transition, as well as determination of the *bubble nucleation temperature* in cosmology is, strictly speaking, beyond the scope of perturbation theory. Indeed, to find the critical temperature one must know not only the value of the potential in the broken minimum, but the value of the potential in the phase with $\phi = 0$. While the first quantity *can* be computed in perturbation theory, the second *cannot*. The same remark applies also to the bubble nucleation temperature, since the computation of the rate of the bubble nucleation requires the knowledge of the effective action for small enough fields ϕ . The determination of these temperatures is impossible in perturbation theory without *additional assumptions* on the behaviour of the potential near the origin. These assumptions are to be checked by non-perturbative methods, say, by lattice Monte Carlo simulations.

Quite an extensive literature exists on the study of the electroweak phase transition (see, e.g. [8]-[24]). A number of papers were devoted to the study of daisy and super-daisy wheel approximations for the effective potential at high temperature, where an attempt to sum up the leading infrared divergencies was made [12]-[15]. The validity of this approximation has been discussed in [19, 15]. A number of important 2-loop contributions to the effective potential have been found in [18, 19]. The large magnitude of these corrections has lead the authors to conclude that the loop expansion for the effective potential is unreliable even for small enough Higgs masses (say, 35 GeV)

³The very high order of the ordinary perturbation theory where this happens often leads to conclusion that these corrections are not important. However, partial resummation of corrections with the help of exact evolution equations [7] reveals that the effective gauge coupling becomes large at $Q^2 \sim (g^2 T/\pi)^2$ making the naive perturbative analysis at these momentum transfers misleading.

[18, 21]. An attempt was made in [21] to overcome this difficulty with the use of the ϵ -expansion.

This paper is the first of two papers devoted to the study of the electroweak phase transition by perturbative and non-perturbative methods. In the present work we apply the method based on the effective field theory approach [25] to the construction of the effective potential at high temperatures. This method reproduces the known 1-loop resummed [10, 11] and 2-loop resummed results [19]-[20] in a very simple and economic way. We show that the conclusion made in refs.[18, 19, 21] on the bad behaviour of the loop expansion due to the presence of large logarithmic corrections is connected with the straightforward use of the minimal subtraction scheme in 4d theory at high temperatures. We point out how to use the renormalization group in 3d to sum up leading logarithms of scalar fields in all orders of perturbation theory and clarify the issue of convergence of perturbation theory. We also discuss the assumptions one can make for the determination of the critical temperature of the EW phase transition, and analyse different perturbative uncertainties in the determination of the critical temperature.

The second paper is devoted to the non-perturbative study of the electroweak phase transition by lattice Monte Carlo methods. We improve there the analysis of [23] in two ways: by going from the 1-loop to the 2-loop level in the discussion of the 3d effective theory and its effective potential and by extending considerably the numerical calculations of [23]. We find at small ϕ considerable deviations from perturbative computations of the effective potential, indicating that the usual assumptions made for the behaviour of the potential near the origin are wrong. We analyse the lattice data in detail and develop further the picture of the electroweak phase transition suggested in [24]. Given the information provided by lattice simulations we re-analyze the question of the Higgs mass necessary for the electroweak baryogenesis [4, 24].

The paper is organized as follows. In section 1 we discuss the advantage of consideration of 3d effective theories for the study of the electroweak phase transition. Section 2 is devoted to the study of renormalization in 3d gauge theories. We present our computation of the 2-loop effective potential in Section 3. In Section 4 we formulate the renormalization group approach to the 3d effective potential. In Section 5 we consider further reduction of 3d gauge theory and relate the theory with the A_0 field to the theory without it. In Section 6 we present 2-loop formulas relating a 4d high temperature theory to a 3d one. Section 7 contains estimates of the parameters of the electroweak phase transition from perturbation theory and discussion of uncertainties. Section 8 is conclusion. Many technical details are discussed in Appendices.

2 Dimensional reduction, dimensional regularization and effective field theories

Electroweak theory at high temperatures contains a number of different mass scales. The largest one is the temperature T itself, then come the Debye screening mass, $m_D \approx gT$ and the ϕ -dependent W mass, $m_W(\phi) = g\phi/2$. For the range of temperatures

relevant for cosmology the following hierarchy of scales holds for small g :

$$T \gg m_D, m_W(\phi). \quad (1)$$

Suppose now that we compute the effective potential for the scalar field in the minimal subtraction scheme⁴. The well known properties of this scheme are that all counterterms in it are polynomials in mass parameters, and that renormalization group equations are mass independent. These properties of the \overline{MS} scheme make *direct* computations with it in theories with many different mass scales practically useless: one has the appearance of logarithms of different scales, say $\log(\mu/m_{\text{small}})$ and $\log(\mu/m_{\text{large}})$, where μ is the unique dimensional parameter in the \overline{MS} scheme. The renormalization group prescription to take μ to be the typical scale in the problem does not work, since it is impossible to kill simultaneously all potentially large logarithms. This problem with the \overline{MS} scheme is well known in the discussion of grand unified theories, heavy quark thresholds, etc. For example, the direct computation of the cross section of the process $e^+e^- \rightarrow \text{hadrons}$ in the \overline{MS} scheme in $SU(5)$ theory at small momenta will immediately lead to the conclusion that the loop expansion does not work due to the presence of large logarithms.

The way out of this problem is well known. One has to use another subtraction scheme, in which heavy particles are decoupled (like the MOM scheme) or use the effective field theory approach in combination with the \overline{MS} scheme [25].

Given the computational advantages of dimensional regularization, we choose the second way. The main idea of the effective field theory approach is the construction of the Lagrangian for light fields which is valid at small momentum transfer by integrating out heavy particle modes [25]. The effective field theory is not renormalizable – though it is finite if one keeps all counterterms of the original theory – but all non-renormalizable terms in the effective lagrangian are suppressed by powers of the large scale. If one is not interested in power corrections of the type $(m_{\text{small}}/m_{\text{large}})^2$, the non-renormalizable terms can be omitted, and the effective lagrangian describes a renormalizable theory. The coupling constants and other parameters like particle masses are to be fixed at the large scale by direct computation in the underlying theory. The effective theory does not contain the heavy scale at all and, therefore, large logarithms of the heavy scale do not appear.

Field theory at finite temperatures provides an example of the theory where integration out of the heavy modes can be very helpful. The euclidean time interval is finite, $0 < \tau < \beta = 1/T$. This allows one to consider 4d field theory at finite temperature as a 3d field theory at zero temperature with an infinite number of excitations with 3d masses $(2\pi nT)^2 + m^2$ for bosons and $((2n + 1)\pi T)^2 + m^2$ for fermions. Then, one can integrate out all fermionic degrees of freedom (they are never massless) and all bosonic modes with $n \neq 0$. This is the dimensional reduction of hot 4d theories [26]-[30].

In order to escape unnecessary complications of the equations we choose to work not in the standard model, but in $SU(2)$ gauge theory with a doublet of scalar fields. This

⁴Everywhere in what follows we use the modified minimal subtraction scheme \overline{MS} . The scale parameter $\bar{\mu}$ in this scheme is related to μ in dimensional regularization through $\bar{\mu}^2 = 4\pi e^{-\gamma} \mu^2$. In order to simplify the notation we use everywhere μ without a bar but meaning the \overline{MS} scheme.

theory has the same problems as the electroweak theory in the infrared region. At the same time, incorporation of fermions does not cause any problems, while the inclusion of the U(1) factor is straightforward but leads to lengthy formulas (see, e.g. [10, 19]).

Just to fix the notations, the 4d lagrangian of the theory under consideration is

$$L = \frac{1}{4}F_{\mu\nu}^a F_{\mu\nu}^a + (D_\mu\phi)^\dagger(D_\mu\phi) - \frac{1}{2}m^2\phi^\dagger\phi + \lambda(\phi^\dagger\phi)^2. \quad (2)$$

We were not able to find in the literature a complete 1-loop analysis of dimensional reduction in this theory. Partial results are contained in the paper by Landsman [28] who has made a computation in the pure SU(N) gauge theory⁵. We present the result of integration of the heavy modes in terms of 3d scalar and vector fields with correct normalization of derivative terms in the \overline{MS} scheme (in order to escape complicated notations we keep the same notation for 4d and 3d fields):

$$S_{\text{eff}}[A_i^a(\mathbf{x}), A_0^a(\mathbf{x}), \phi_i(\mathbf{x})] = \int d^3x \left\{ \frac{1}{4}F_{ij}^a F_{ij}^a + \frac{1}{2}(D_i A_0)^a (D_i A_0)^a + (D_i\phi)^\dagger(D_i\phi) + \frac{1}{2}m_D^2 A_0^a A_0^a + \frac{1}{4}\lambda_A (A_0^a A_0^a)^2 + m_3^2\phi^\dagger\phi + \lambda_3(\phi^\dagger\phi)^2 + h_3 A_0^a A_0^a \phi^\dagger\phi \right\}. \quad (3)$$

Here all bosonic fields have the canonical dimension $[\text{GeV}]^{\frac{1}{2}}$ and 3d gauge and scalar couplings g_3^2 , λ_3 , λ_A and h_3 have dimension $[\text{GeV}]$. These parameters and the masses m_3 and m_D can be expressed in terms of 4d couplings and the temperature as follows:

$$g_3^2 = g^2(\mu)T \left[1 + \frac{g^2 L_s}{(4\pi)^2} \left(\frac{22}{3} - \frac{1}{6}N_s \right) \right], \quad (4)$$

$$\lambda_3 = T \left[\lambda(\mu) - \frac{L_s}{(4\pi)^2} \left(\frac{9}{16}g^4 - \frac{9}{2}\lambda g^2 + 12\lambda^2 \right) + \frac{1}{(4\pi)^2} \frac{3}{8}g^4 \right], \quad (5)$$

$$h_3 = \frac{1}{4}g^2(\mu)T \left[1 + \frac{g^2 L_s}{(4\pi)^2} \left(\frac{22}{3} - \frac{1}{6}N_s \right) + \frac{1}{(4\pi)^2} \left(12\lambda + \frac{49}{6}g^2 - \frac{1}{3}g^2 N_s \right) \right] = \quad (6)$$

$$\frac{1}{4}g_3^2 \left[1 + \frac{1}{(4\pi)^2} \left(12\lambda + \frac{49}{6}g^2 - \frac{1}{3}g^2 N_s \right) \right],$$

$$\lambda_A = \frac{17g^4(\mu)T}{48\pi^2}, \quad (7)$$

$$m_D^2 = \frac{5}{6}g^2(\mu)T^2, \quad (8)$$

$$m_3^2 = \left[\frac{3}{16}g^2(\mu) + \frac{1}{2}\lambda(\mu) \right] T^2 - \frac{1}{2}m^2(\mu) \left[1 + \frac{L_s}{(4\pi)^2} \left(-\frac{9}{4}g^2 + 6\lambda \right) \right], \quad (9)$$

⁵Some of the equations in the appendix of [28] must be taken with care. For example, eq.(A.7), as it appears in that paper is not correct. We suspect that this is due to a misprint, since we checked a number of terms in the final equation (6.3) with the use of correct version of (A.7), and found a result coinciding with (6.3) of [28].

where

$$L_s = 2 \log \frac{\mu e^\gamma}{4\pi T} = \log \frac{\mu^2}{T^2} - 2c_B, \quad c_B = \log(4\pi) - \gamma, \quad (10)$$

γ is the Euler constant, μ is the scale parameter of the \overline{MS} scheme and $N_s = 1$ is the number of the scalar doublets. Note the systematic appearance of the constant c_B in thermal dimensional reduction. We stress that all relations between coupling constants and masses are gauge invariant (but may be scheme dependent).

The expressions of 3d fields in terms of bare 4d fields are gauge dependent, and we present them in Landau gauge. A number of terms can be found in [28], we have added the contribution of scalars:

$$\phi^{3d} = \frac{1}{\sqrt{T}} \phi \left(1 - \frac{g^2}{(4\pi)^2} \frac{9}{8} \frac{1}{\epsilon_B} \right), \quad (11)$$

$$A_0^{3d} = \frac{1}{\sqrt{T}} A_0 \left[1 + \frac{g^2}{(4\pi)^2} \left(\frac{5}{3} - \frac{13}{6} \frac{1}{\epsilon_B} + \frac{1}{12} N_s \left(\frac{1}{\epsilon_B} + 2 \right) \right) \right], \quad (12)$$

$$A_i^{3d} = \frac{1}{\sqrt{T}} A_i \left[1 + \frac{g^2}{(4\pi)^2} \left(-\frac{13}{6} \frac{1}{\epsilon_B} + \frac{1}{12} N_s \frac{1}{\epsilon_B} \right) \right]. \quad (13)$$

Here

$$1/\epsilon_B = 1/\epsilon + L_s. \quad (14)$$

We note that the constants g_3 , λ_3 , h_3 as well as the term proportional to m^2 in eq. (9) do not depend on the parameter μ up to higher order terms in coupling constants. The reason is that the coefficients in front of the logarithm L_s are just the corresponding β -functions. This is not surprising, as we will see in the next section. To this order of perturbation theory there are no corrections proportional to $\log(\mu/T)$ to eqs. (7,8) or to the term proportional to T^2 in eq. (9). They can appear on the 2-loop level of dimensional reduction, see Section 6. (We stress that no logs of the type $\log(\mu/m)$ can appear when one integrates out heavy modes!) By the choice

$$\mu = \mu_T = 4\pi T e^{-\gamma} \sim 7T \quad (15)$$

all logarithmic contributions can be removed. In loose terms, μ_T is an average momentum of integration of heavy modes. Perturbation theory for the *construction of the effective 3d theory from the 4d one* is valid only when logarithmic corrections are small, i.e. with the choice of parameter $\mu \sim \mu_T$. So, we have the explicitly μ independent relations⁶

$$\begin{aligned} g_3^2 &= g^2(\mu_T) T, \\ \lambda_3 &= T \left[\lambda(\mu_T) + \frac{1}{(4\pi)^2} \frac{3}{8} g^4(\mu_T) \right], \\ h_3 &= \frac{1}{4} g_3^2 \left[1 + \frac{1}{(4\pi)^2} \left(12\lambda(\mu_T) + \frac{49}{6} g^2(\mu_T) - \frac{1}{3} g^2(\mu_T) N_s \right) \right], \end{aligned}$$

⁶Of course, the use of, e.g. $g(\mu_T)$ instead of $g(\mu)$ in the one-loop terms goes beyond the assumed accuracy, but is not essential numerically.

$$\lambda_A = \frac{17g^4(\mu_T)T}{48\pi^2}, \quad (16)$$

$$m_D^2 = \frac{5}{6}g^2(\mu_T)T^2,$$

$$m_3^2 = \left[\frac{3}{16}g^2(\mu_T) + \frac{1}{2}\lambda(\mu_T)\right]T^2 - \frac{1}{2}m_H^2, \quad m_H^2 \equiv m^2(\mu_T).$$

Note that the coupling between A_0 and ϕ is not the same as the coupling between A_i and ϕ . The reason is the absence of the Lorentz invariance at non-zero temperatures. The difference, however, is very small, less than 3% for Higgs masses < 80 GeV. In order to escape unnecessary complications of the equations we use in what follows

$$h_3 = \frac{1}{4}g_3^2 \quad (17)$$

instead of (6).

Our aim is the construction of the effective potential at sufficiently small ϕ , so that particle masses coming from the Higgs mechanism are much smaller than μ_T . This should be done *in effective 3d theory*, since the direct use of perturbation theory and the \overline{MS} scheme for the effective potential at small ϕ in the underlying 4d theory will immediately give rise to large logs. According to the philosophy of the effective theories [25] the equations (16) are to be used as boundary conditions for the determination of the parameters of our 3d theory at small momenta (or, equally, fields ϕ).

The dimensional reduction of 4d gauge theory produces non-renormalizable as well as renormalizable (in 3d) higher order terms not included above. The relevant coupling constants are suppressed by powers of temperature and by numerical constants. The terms $\sim 1/T^3$ have been computed in [31]. For example, the higher order term $\phi^\dagger\phi(A_0^a A_0^a)^2$ is multiplied by $-\zeta(3)g_3^6/(64\pi^4 T^3)$. The coefficient of the renormalizable term $\sim (A_0^a A_0^a)^3$ vanishes in SU(2) gauge theory but equals [28] $\frac{889\zeta(3)\epsilon^6}{6144\pi^4}$ in quantum electrodynamics. It is clear that the presence of these small terms cannot change the character of infrared phenomena we are interested in.

In Sections 3–7 we will study in more detail the 3d effective theory defined in (3).

3 Peculiarities of renormalization of 3d theory

Until Section 5 we shall forget the 4d origin of our 3d theory and study it as it stands as a 3d SU(2) gauge theory with a fundamental Higgs field ϕ and an adjoint Higgs field A_0 . On the tree level our theory (3) is characterized by the six parameters $m_3, m_D, \lambda_A, \lambda_3, h_3$ and g_3^2 . This 3d theory is super-renormalizable. There are a finite number of irreducible graphs which are ultraviolet divergent. One-loop diagrams are presented in Fig. 1, and 2-loop diagrams in Figs. 2 (δm^2) and 3 (δm_D^2). One-loop graphs are linearly divergent while 2-loop graphs are logarithmically divergent. All these diagrams correspond to the mass renormalization of the triplet and doublet Higgs fields. As usual in quantum field theory the appearance of logarithmic divergencies introduces an extra scale, μ_3 . For concreteness, we choose μ_3 to be the scale

parameter in the modified minimal subtraction scheme \overline{MS} , associated with dimensional regularization. We stress that at this stage the parameter μ_3 introduced here has nothing to do with the parameter μ introduced previously in the discussion of dimensional reduction. The change in the parameter μ_3 changes the physical content of the theory unless tree parameters are varied with μ_3 in some consistent way, given by renormalization group equations. In our case only mass diagrams contain logarithmic divergencies, so that the coupling constants λ_A , λ_3 , h_3 and g_3^2 are 3d renormalization group invariants. This is the reason for the appearance of the β -functions in eqs.(4-9) of the previous section. Just on dimensional grounds one can write the following renormalization group equations for the mass parameters:

$$\mu_3 \frac{\partial m_3^2(\mu_3)}{\partial \mu_3} = -\frac{1}{16\pi^2} f_{2m}, \quad \mu_3 \frac{\partial m_D^2(\mu_3)}{\partial \mu_3} = -\frac{1}{16\pi^2} f_{2D}, \quad (18)$$

where f_{2m} and f_{2D} are second order polynomials in coupling constants. We stress that these equations are exact due to the super-renormalizable character of 3d gauge theory. Generally, to make a theory finite, one has to add mass counterterms to the action (3),

$$\delta S = \int d^3x \left\{ \delta m^2 \phi^\dagger \phi + \frac{1}{2} \delta m_D^2 A_0^a A_0^a \right\}, \quad (19)$$

where

$$\delta m^2 = f_{1m} \Sigma + f_{2m} \Sigma_{\log}, \quad \delta m_D^2 = f_{1D} \Sigma + f_{2D} \Sigma_{\log}, \quad (20)$$

where f_{1m} and f_{1D} are first order polynomials in coupling constants. The quantity Σ is related to the following linearly divergent integral

$$\int \frac{d^3p}{(2\pi)^3} \frac{1}{\mathbf{p}^2 + m^2}. \quad (21)$$

Clearly, it depends on the regularization scheme. In the momentum regularization scheme (Λ is an UV cutoff) $\Sigma = \Lambda/2\pi^2$, in lattice regularization $\Sigma = 0.252731/a$ with a being the lattice spacing, and $\Sigma = 0$ in the minimal subtraction scheme \overline{MS} . The quantity Σ_{\log} is related to the logarithmically divergent 2-loop sunset diagram ($d = 3 - 2\epsilon$)

$$\begin{aligned} H(m_1, m_2, m_3) &= \mu_3^{4\epsilon} \int \frac{d^d p}{(2\pi)^d} \frac{d^d k}{(2\pi)^d} \frac{1}{(\mathbf{p}^2 + m_1^2)(\mathbf{k}^2 + m_2^2)(|\mathbf{p} + \mathbf{k}|^2 + m_3^2)} = \\ &= \frac{1}{64\pi^2 \epsilon} + \frac{1}{(4\pi)^2} \left(\log \frac{\mu_3}{m_1 + m_2 + m_3} + \frac{1}{2} \right). \end{aligned} \quad (22)$$

Again, in momentum regularization

$$\Sigma_{\log} = \frac{1}{16\pi^2} \left(\log \frac{\Lambda}{\mu_3} - \frac{1}{2} \right), \quad (23)$$

in the minimal subtraction scheme

$$\Sigma_{\log} = \frac{1}{64\pi^2 \epsilon}, \quad (24)$$

and on the lattice a numerical estimate of the sunset graph gives

$$\Sigma_{log} = \frac{1}{16\pi^2} \left(\log \frac{6}{a\mu_3} + 0.09 \right). \quad (25)$$

The constant finite terms in these expressions are defined in such a way that after renormalization the value of the sunset graph is the same for all renormalization schemes we discussed.

For a number of applications (in particular for the analysis of the lattice data) the knowledge of the counterterms is a must. A direct computation with the use of the relation (17) gives:

$$f_{1m} = -\left(\frac{9}{4}g_3^2 + 6\lambda_3\right), \quad f_{1D} = -5(g_3^2 + \lambda_A), \quad (26)$$

and for the logarithmic counterterms

$$f_{2m} = \frac{81}{16}g_3^4 + 9\lambda_3g_3^2 - 12\lambda_3^2, \quad f_{2D} = 5\lambda_A^2 - 20g_3^2\lambda_A. \quad (27)$$

The expressions for f_{1m} , f_{2m} , f_{1D} and f_{2D} are *exact* and do not have any higher order corrections. The derivation of eqs. (27) is given in Appendix A. It is also quite interesting to express f_{2m} as a function of m_H using the tree relations $g_3^2 = g^2T$, $\lambda_3 = \lambda T$, $\lambda = g^2m_H^2/(8m_W^2)$:

$$f_{2m} \propto \left[1 - \left(\frac{m_H}{3m_W} \right)^2 \right] \left[3 \left(\frac{m_H}{3m_W} \right)^2 + 1 \right]. \quad (28)$$

It thus vanishes for $m_H = 3m_W$!

To summarize, the theory under consideration is characterized by two renormalization invariant scales Λ_m and Λ_D , and three independent coupling constants g_3^2 , λ_3 and λ_A (since we used relation between h_3 and g_3)⁷. The relations between lagrangian masses and renormalization invariant scales are given by

$$m_3^2(\mu_3) = \frac{1}{16\pi^2} f_{2m} \log \frac{\Lambda_m}{\mu_3}, \quad m_D^2(\mu_3) = \frac{1}{16\pi^2} f_{2D} \log \frac{\Lambda_D}{\mu_3}, \quad (29)$$

Quite an interesting situation arises when $\lambda_A = 0$. Then there is no 2-loop counter term for the A_0 mass term ($f_{2D} = 0$), the various diagrams in Fig. 2 cancel each other. Furthermore, this cancellation also takes place in a 3d theory even without the doublet Higgs field. So, in this case m_D^2 is a renormalization invariant quantity (μ_3 independent). In fact the relation $\lambda_A = 0$ is almost true for a three dimensional theory derived by dimensional reduction from 4d high temperature one, since according to (7) $\lambda_A \sim 1.6 \cdot 10^{-2} g_3^2$. For a realistic choice of SU(2) gauge coupling $g = 2/3$ this is numerically much smaller than all other couplings. These can as above be estimated, say, from $\lambda_3 = m_H^2/(8m_W^2)g_3^2$. For QCD clearly g and correspondingly λ_A will be much larger and it is possible that 2-loop counterterms could modify the studies of dimensional reduction in hot QCD in [29]-[30].

⁷We stress that these relations are not spoiled by the renormalization due to super-renormalizable character of 3d theory.

4 The effective potential of the 3d theory to 2 loops

The object which is used for the study of the phase transitions is the effective potential [32]. As usual for gauge theories, the effective potential is gauge dependent. We use the Landau gauge and dimensional regularization for all our computations.

In the 1-loop approximation the effective potential for the scalar field in the effective 3d theory defined by the action in eq. (3) was given in [23]. We define the mean field dependent masses as

$$\begin{aligned} m_T &= \frac{1}{2}g_3\phi, & m_L^2 &= m_D^2 + \frac{1}{4}g_3^2\phi^2, \\ m_1^2 &= m_3^2(\mu_3) + 3\lambda_3\phi^2, & m_2^2 &= m_3^2(\mu_3) + \lambda_3\phi^2 \end{aligned} \quad (30)$$

Then the 1-loop potential is

$$\begin{aligned} V_1(\phi) &= \frac{1}{2}m_3^2(\mu_3)\phi^2 + \frac{1}{4}\lambda_3\phi^4 - \\ &\quad - \frac{1}{12\pi} \left(6m_T^3 + 3m_L^3 + m_1^3 + 3m_2^3 \right). \end{aligned} \quad (31)$$

As one could expect, this potential coincides with the high temperature expansion of potential in the daisy wheel approximation found in a number of papers [10] -[14]. The 1-loop computation of the effective potential cannot fix the arbitrary scale μ_3 appearing as the argument in the scalar mass⁸. For physical reasons it is clear, though, that in order to minimize higher order corrections this scale should be of the order of particle masses defined by eq. (30). We will return to the discussion of this question later.

To fix the scale μ_3 we must compute the 2-loop potential. The relevant diagrams are given in Fig. 4 and the computation is carried out in considerable detail in Appendix B. Using the function

$$\bar{H}(m_1, m_2, m_3) = \log \frac{\mu_3}{m_1 + m_2 + m_3} + \frac{1}{2} \quad (32)$$

the result for the 2-loop contribution to the potential in dimensional regularization is

$$\begin{aligned} V_2(\phi, \mu_3) &= \frac{1}{16\pi^2} \left\{ \right. \\ &\quad - \frac{3g_3^4}{16} \phi^2 \left[2\bar{H}(m_1, m_T, m_T) - \frac{1}{2}\bar{H}(m_1, m_T, 0) + \bar{H}(m_1, m_L, m_L) \right] \\ &\quad + \frac{m_1^2}{m_T^2} [\bar{H}(m_1, m_T, 0) - \bar{H}(m_1, m_T, m_T)] \\ &\quad + \frac{m_1^4}{4m_T^4} [\bar{H}(m_1, 0, 0) + \bar{H}(m_1, m_T, m_T) - 2\bar{H}(m_1, m_T, 0)] \end{aligned}$$

⁸The effective potential in the 1-loop approximation is renormalization invariant only up to terms of the order of g_3^4 , $g_3^2\lambda_3$ and λ_3^2 .

$$\begin{aligned}
& -\frac{m_1}{2m_T} - \frac{m_1^2}{4m_T^4} \Big] \\
& -3\lambda_3^2\phi^2[\bar{H}(m_1, m_1, m_1)\bar{H}(m_1, m_2, m_2)] \\
& +2g_3^2m_T^2\left[\frac{63}{16}\bar{H}(m_T, m_T, m_T) + \frac{3}{16}\bar{H}(m_T, 0, 0) - \frac{41}{16}\right] \\
& -\frac{3}{2}g_3^2[(m_T^2 - 4m_L^2)\bar{H}(m_L, m_L, m_T) - 2m_Tm_L - m_L^2] \\
& +4g_3^2m_T^2 + \frac{3}{8}g_3^2(2m_T + m_L)(m_1 + 3m_2) \\
& +\frac{15}{4}\lambda_A m_L^2 + \frac{3}{4}\lambda_3(m_1^2 + 2m_1m_2 + 5m_2^2) \\
& -\frac{3}{8}g_3^2[(m_T^2 - 2m_1^2 - 2m_2^2)\bar{H}(m_1, m_2, m_T) + (m_T^2 - 4m_2^2)\bar{H}(m_2, m_2, m_T) \\
& +\frac{(m_1^2 - m_2^2)^2}{m_T^2}[\bar{H}(m_1, m_2, m_T) - \bar{H}(m_1, m_2, 0)] \\
& + (m_1^2 - m_2^2)(m_1 - m_2)/m_T + m_T(m_1 + 3m_2) - m_1m_2 - m_2^2] \Big\}.
\end{aligned} \tag{33}$$

The logarithmically divergent 2-loop counter term in eq.(27) can be directly extracted from eq.(33): the coefficient $f_{2m} = 81g_3^4/16 + 9\lambda_3g^2 - 12\lambda_3^2$ is simply the sum of the coefficients of the $\frac{1}{2}\phi^2\bar{H}$ - terms within the braces there. The derivation of eq. (33) is quite lengthy but it is still much more straightforward than that in the 4d case at non-zero temperatures [19]-[20]⁹.

The total 2-loop effective potential, normalized to zero,

$$V_{\text{tot}} = V_1(\phi) + V_2(\phi) - V_1(0) - V_2(0), \tag{34}$$

is now renormalization invariant up to the higher order terms in the gauge and scalar self-coupling constants. Due to the fact that the ultraviolet renormalization of any of the wave functions of the fields in our 3d theory is absent, the exact effective potential, normalized as in (34), is renormalization group invariant.

In what follows, we will put for simplicity $\lambda_A = 0$, since its numerical value is small. However, the more general case can be treated also without any problems.

5 Renormalization group and convergence of perturbation theory

There are two aspects of the convergence of perturbation theory in 3d. The first problem is associated with ultraviolet logarithmic renormalization. As far as we know it has not been discussed in the literature in the present context. The second one is the

⁹Shortly after our paper was completed the paper by Z. Fodor and A. Hebecker (Preprint DESY 94-025) appeared where the authors computed the high temperature asymptotic of the two-loop effective potential accounting for λ^2 and $g^2\lambda$ terms. Due to different normalization conditions we were not able to compare our results.

well known infrared problem. In spite of the fact that this problem has been discussed already in a number of papers, we will discuss it too in the Section 7, adding some new views and estimates.

5.1 Preliminaries

Since the 1-loop as well as the 2-loop effective potentials depend explicitly on the scale μ_3 , while the exact effective potential is μ_3 independent, the question of the convergence of perturbation theory must be formulated accounting for this fact. Let us discuss this in more detail.

Clearly, this type of situation is not new. It arises in any calculation in any quantum field theory containing logarithmic divergencies, in particular in QCD or QED. For example, the cross-section of, say, gluon-gluon scattering in the tree approximation is proportional to $\alpha_s^2(\mu)$ and *is not defined* at all without the fixing of the scale μ . The method of dealing with this problem is, of course, well known. It is a *combination* of the perturbation theory and *renormalization group*, which sums up leading logarithmic corrections. In our example with gluon scattering one simply says that $\mu^2 \sim Q^2$, where Q^2 is a typical momentum transfer and uses a 1-loop running coupling α_s . Then, 1-loop corrections to the process do not contain any logarithms of the type $\log(Q^2/\mu^2)$, so that the expansion proceeds in powers of $\alpha_s(Q^2)$ rather than of the quantity $\alpha_s(\mu)$. The question of the convergence of perturbation theory becomes therefore more complicated. In particular, for the processes depending on just one energy scale, the parameter μ may be chosen in such a way that 1-loop corrections to a tree result simply vanish. Suppose this happens at some $\mu^2 = \kappa Q^2$. Then the QCD folklore says that perturbation theory works if $\alpha_s(\kappa Q^2)/\pi \ll 1$. In order to check the convergence of perturbation theory, one has to go generally to a 2-loop level.

Of course, our 3d theory is different from theories in 4 dimensions. Our gauge and scalar couplings do not run. The only quantity depending on the scale μ_3 is the mass of the scalar doublet. It has a qualitatively different behaviour depending on the parameters of the theory. As seen from eqs. (28-29), for small scalar self-coupling (corresponding to $m_H < 3m_W$) $m_3^2(\mu_3)$ is positive at small μ_3 and negative at large μ_3 , while for $m_H > 3m_W$ the situation is opposite. The point $m_H = 3m_W$ is quite specific, for this value of the Higgs mass logarithmic renormalization is absent. It is interesting to note that in the abelian Higgs model $f_{2m} = -6g_3^4[1 - 2m_H^2/(3m_W^2) + m_H^4/(3m_W^4)]$ is always negative independently of the mass of the Higgs boson (see Appendix B.3).

5.2 Example: The scalar theory

In order to understand in more detail how the μ_3 dependence should be dealt with, we take first a simplest possible example, namely ϕ^4 theory in 3d, defined by the Lagrangian

$$\mathcal{L} = \frac{1}{2}(\partial_i\phi)^2 + \frac{1}{2}m_3^2\phi^2 + \frac{1}{4}\lambda_3\phi^4. \quad (35)$$

This theory is super-renormalizable and in the dimensional regularization scheme there is only one divergent graph, namely the sunset diagram contributing to the mass of the scalar field. The 2-loop effective potential, derived in detail in Appendix B.1, is:

$$V_{\text{eff}}(\phi) = \frac{1}{2}m^2(\mu_3)\phi^2 + \frac{1}{4}\lambda_3\phi^4 - \frac{1}{12\pi}m_1^3(\phi) + \frac{\lambda_3}{64\pi^2}3m_1^2(\phi) - 3\frac{\lambda_3^2}{16\pi^2}\left(\log\frac{\mu_3}{3m_1(\phi)} + \frac{1}{2}\right)\phi^2, \quad (36)$$

where $m_1(\phi)^2 = m^2(\mu_3) + 3\lambda_3\phi^2$ and

$$m^2(\mu_3) = 3\frac{\lambda_3^2}{8\pi^2}\log\frac{\mu_3}{\Lambda_m}. \quad (37)$$

The 3d theory depends on the parameters λ_3 and Λ_m . The former is related to the 4d λ via equation similar to (5). We shall in Section 6 give Λ_m in terms of T .

Due to the μ_3 dependence of $m(\mu_3)$, the 2-loop effective potential is, in fact, μ_3 independent up to 3-loop corrections. The scale μ_3 can thus be chosen at will and should be chosen so as to minimize the effect of large logarithms. For example, one may require that two-loop contribution to the effective potential vanishes. In our case this happens at $\mu_3 = 3\exp(1/4)m_1(\phi)$. This simple prescription, however, is not absolutely correct. The reason is that the effective potential itself is not a good object for renormalization group studies. It is not a measurable physical quantity – only the difference

$$V(\phi_1) - V(\phi_2) \quad (38)$$

has physical meaning. The potential is defined up to an additive constant. In fact in the minimal subtraction scheme this constant is μ_3 -dependent, so that the potential itself (not normalized to zero at $\phi = 0$) is not a renormalization group invariant. If ϕ_1 and ϕ_2 are very different from each other, then characteristic momenta of integration defining $V(\phi_1)$ and $V(\phi_2)$ are different, and renormalization group improvement is not possible. The simplest way to solve this problem is to consider the derivative of the effective potential,

$$DV(\phi) \equiv dV/d\phi \quad (39)$$

which must be μ_3 independent. Moreover, the loop integration momenta are defined by a single scale, $p \sim m(\phi)$.

The renormalization group equation is trivial:

$$\left(\mu_3\frac{\partial}{\partial\mu_3} - \frac{1}{16\pi^2}f_{2m}\frac{\partial}{\partial m^2}\right)DV(\phi, \mu_3, m^2) = 0. \quad (40)$$

The summation of the leading logs will be achieved with the choice of

$$\mu_3 = 3\kappa m_1(\phi), \quad (41)$$

after first taking the derivative with respect to ϕ , where κ is a constant determined by some criterion of minimizing 2-loop effects. For example, one may require the value

of ϕ at the broken minimum at T_c to be equal for the 1- and 2-loop potentials. The renormalization group improved expression for the effective potential is therefore

$$V_{\text{rg}}(\phi) = \int_0^\phi d\phi DV(\phi, \mu_3, m^2(\mu_3))|_{\mu_3=3\kappa m_1(\phi)}. \quad (42)$$

with κ being a number of order of one.

In fact, the knowledge of the effective potential up to two loops allows one to compute 3- and 4-loop logarithmic terms with the help of the renormalization group. Because of the μ_3 dependence of $m_1(\phi)$, there in V_1 is a μ_3 dependence $\mu_3 \partial V_1 / \partial \mu_3$ which is of 3-loop order. For the 3-loop potential to satisfy $\mu_3 \partial V_3 / \partial \mu_3 = 0$ it must contain a compensating logarithmic term $-\mu_3 \partial V_1 / \partial \mu_3 \times \log[\mu_3 / m_1(\phi)]$. Thus the logarithmic term in the 3-loop correction to the potential is

$$\Delta V_3 = -\mu_3 \frac{\partial V_1(\phi)}{\partial \mu_3} \log \frac{\mu_3}{m_1(\phi)} = \frac{1}{12\pi} \mu_3 \frac{\partial m_1^3(\phi)}{\partial \mu_3} \log \frac{\mu_3}{m_1(\phi)} = \frac{3\lambda_3^2}{(4\pi)^3} m_1(\phi) \log \frac{\mu_3}{m_1(\phi)}. \quad (43)$$

Similarly, the 4-loop correction must contain the logarithmic term

$$\Delta V_4 = -\frac{\partial V_2}{\partial m^2} \mu_3 \frac{\partial m^2}{\partial \mu_3} \log \frac{\mu_3}{m_1(\phi)} = -\frac{3\lambda_3^3}{(4\pi)^4} \left[\frac{5}{2} - \frac{m^2}{m_1^2(\phi)} \right] \log \frac{\mu_3}{m_1(\phi)}. \quad (44)$$

The comparison of, say, 2-loop and 3-loop logarithmic terms gives an idea of when renormalization group improved perturbation theory works, namely for

$$m_1(\phi) \gg \frac{\lambda_3}{4\pi} \quad (45)$$

where μ_3 is chosen in accordance with (41).

The summary of this exercise is as follows. Due to the μ_3 -dependence of the scalar mass tree and 1-loop potentials do not have definite sense, since any result obtained with them contains unphysical μ_3 dependence. The scale μ_3 can be fixed from the requirement that the contribution of 2-loop diagrams is minimized. This happens when μ_3 is of the order of a typical scale in the problem, namely the ϕ dependent scalar mass. In the 2-loop effective potential μ_3 dependence appears on the 3-loop level. The effective summation of the leading logs can be achieved with a choice of μ_3 in accordance with eq.(41) on the level of 2-loop effective potential.

5.3 SU(2) theory

The general remarks applicable to the pure scalar model are also valid for SU(2). Namely, the 1-loop effective potential does not have a definite sense without fixing of the scale μ_3 . The dependence of the 2-loop effective potential on μ_3 appears on the 3-loop level. However, the choice of μ_3 is not so evident as in the previous case. The reason is that we have now several different scales in the problem, namely four different masses (m_1 and m_2 for Higgses, m_T for the gauge boson and m_L for the adjoint Higgs

field). For the applications to a realistic electroweak theory two cases are the most interesting.

The first one is the case when the Higgs mass is so small that the Higgs contributions to the effective potential are suppressed by the small scalar self-coupling constants and may be neglected. Then basically only m_T and m_L appear in the logs (this happens also when the Higgs mass is of the order of W mass, so that remarks below are applicable to this case as well). The natural guess is to take μ_3 such that the sum of all 2-loop logarithmic corrections vanishes. Neglecting scalar masses we get

$$\mu_3 = \kappa m_L(\phi)^{1-\zeta} m_T(\phi)^\zeta \equiv \mu(\phi) \quad (46)$$

with

$$\zeta = \frac{f_{2m}^0}{f_{2m}}, \quad (47)$$

where f_{2m}^0 is to be computed in a theory without the triplet Higgs field A_0^a (see Section 5.4 and Appendix B.4):

$$f_{2m}^0 = \frac{51}{16} g_3^4 + 9\lambda_3 g_3^2 - 12\lambda_3^2, \quad (48)$$

and κ is some arbitrary parameter, $\kappa \sim 1$. While this choice is certainly good for the minimization of the 2-loop corrections, one may wonder if it is good for the higher order terms. Later we will provide more motivation for this choice, coming from the consideration of an effective theory with the A_0^a field integrated out.

So, we define a renormalization group improved effective potential in a perfect analogy with (42),

$$V_{\text{rg}}(\phi) = \int_0^\phi d\phi DV(\phi, \mu_3, m^2(\mu_3))|_{\mu_3=\mu(\phi)}. \quad (49)$$

where DV is a partial derivative of the 1- or 2-loop effective potential with respect to ϕ .

The 2-loop effective potential depends on the scale μ_3 only weakly. The same is true for the dependence on κ of the renormalization group improved effective potential derived in the 2-loop approximation. The 1-loop improved effective potential depends on κ strongly. The minimal sensitivity requirement would be to choose κ in such a way that the minimum of the 1-loop effective potential is at the same point as for 2-loop potential.

The second case is when the Higgs mass is so large that m_1 and m_2 appearing in the log terms are greater than the vector boson mass. Then the parameter μ_3 should be associated with the scalar masses. We will not consider this case, since it is expected that the electroweak phase transition is weakly first order in this region.

5.4 Integrating out the A_0 field

Going from 4 to 3 dimensions we were able to escape the problem of large logs of the type $\log(T/m_L)$ and $\log(T/m_T)$. However, if $m_T \ll m_L$, then logs of the type $\log(\mu_3/m_L)$ and $\log(\mu_3/m_T)$ will appear on the level of 3d theory as well. The effective

theories provide again the recipe of the summation. One has just integrate out the A_0 field and construct a new effective theory (see Appendix B.4).

The new effective action in the 1-loop approximation is

$$S_{\text{eff}}[A_i^a(\mathbf{x}), \phi_i(\mathbf{x})] = \int d^3x \left\{ \frac{1}{4} F_{ij}^a F_{ij}^a + (D_i \phi)^\dagger (D_i \phi) + \bar{m}_3^2 \phi^\dagger \phi + \bar{\lambda}_3 (\phi^\dagger \phi)^2 \right\}. \quad (50)$$

There is no wave function renormalization coming from A_0 integration and the connection between new and old parameters on the 1-loop level is

$$\bar{g}_3^2 = g_3^2 \left(1 - \frac{g_3^2}{24\pi m_D} \right), \quad (51)$$

$$\bar{\lambda}_3 = \lambda_3 - \frac{3g_3^4}{128\pi m_D}, \quad (52)$$

$$\bar{m}_3(\mu_3)^2 = m_3^2(\mu_3) - \frac{3g_3^2 m_D}{16\pi} + \frac{15g_3^4}{8(4\pi)^2} \left(\log \frac{\mu_3}{2m_D} + \frac{3}{10} \right). \quad (53)$$

The last term in the $\bar{m}_3^2(\mu_3)$ removes the heavy A_0 degrees of freedom from the renormalization group equation, i.e., replaces f_{2m} by f_{2m}^0 defined in eq. (48). We shall derive the above relations in Appendix B.4 by considering the $m_D \rightarrow \infty$ limit of the 2-loop potential. The 2-loop effective potential for the theory defined by (50) can be extracted from (33) just by dropping the A_0 contributions and relating the parameters by eqs.(51-53). We present the result for completeness:

$$\begin{aligned} V(\phi) &= \frac{1}{2} \bar{m}_3^2(\mu_3) \phi^2 + \frac{1}{4} \bar{\lambda} (\phi^2)^2 \\ &- \frac{1}{12\pi} (6m_T^3 + m_1^3 + 3m_2^3) + \frac{1}{16\pi^2} \left\{ \right. \\ &- \frac{3\bar{g}_3^4}{16} \phi^2 \left[2\bar{H}(m_1, m_T, m_T) - \frac{1}{2} \bar{H}(m_1, m_T, 0) \right. \\ &\quad \left. + \frac{m_1^2}{m_T^2} [\bar{H}(m_1, m_T, 0) - \bar{H}(m_1, m_T, m_T)] \right. \\ &\quad \left. + \frac{m_1^4}{4m_T^4} [\bar{H}(m_1, 0, 0) + \bar{H}(m_1, m_T, m_T) - 2\bar{H}(m_1, m_T, 0)] \right. \\ &\quad \left. \left. - \frac{m_1}{2m_T} - \frac{m_1^2}{4m_T^4} \right] \right. \\ &- 3\bar{\lambda}_3^2 \phi^2 [\bar{H}(m_1, m_1, m_1) + \bar{H}(m_1, m_2, m_2)] \\ &\left. + 2\bar{g}_3^2 m_T^2 \left[\frac{63}{16} \bar{H}(m_T, m_T, m_T) + \frac{3}{16} \bar{H}(m_T, 0, 0) - \frac{41}{16} \right] - \right. \\ &\left. + 4\bar{g}_3^2 m_T^2 + \frac{3}{4} \bar{g}_3^2 m_T (m_1 + 3m_2) + \frac{3}{4} \bar{\lambda}_3 (m_1^2 + 2m_1 m_2 + 5m_2^2) \right. \\ &\left. - \frac{3}{8} \bar{g}_3^2 [(m_T^2 - 2m_1^2 - 2m_2^2) \bar{H}(m_1, m_2, m_T) + (m_T^2 - 4m_2^2) \bar{H}(m_2, m_2, m_T)] \right. \\ &\left. + \frac{(m_1^2 - m_2^2)^2}{m_T^2} [\bar{H}(m_1, m_2, m_T) - \bar{H}(m_1, m_2, 0)] \right\} \end{aligned} \quad (54)$$

$$+(m_1^2 - m_2^2)(m_1 - m_2)/m_T + m_T(m_1 + 3m_2) - m_1m_2 - m_2^2] \},$$

The mass parameters appearing in this expression are to be computed with the help of eq. (30) and substitution $g_3 \rightarrow \bar{g}_3$, $\lambda_3 \rightarrow \bar{\lambda}_3$, $m_3 \rightarrow \bar{m}_3$. To get a renormalization group improved potential one now just chooses $\mu_3 \sim m_T$ in the effective theory without the A_0 field and uses (49). Note that due to (53) this choice of μ_3 corresponds to (46). Again, no large logs will appear. We note also that this procedure sums up in all orders of perturbation theory A_0 ring insertions.

Now we are ready to discuss the relation between high temperature 4d and 3d physics on the 2-loop level.

6 The relation between 3d and 4d computations on the 2-loop level

In Section 2 we have derived the parameters of the effective 3d theory in terms of the 4d parameters by explicit integration over the nonstatic modes of the 4d theory. However, the calculation is not yet complete: due to 3d renormalization the mass parameters are of the form

$$m_3^2(\mu_3) = \frac{1}{16\pi^2} f_{2m} \log \frac{\Lambda_m}{\mu_3}, \quad (55)$$

and we still have to express the scale Λ_m in terms of T . This can be done by comparing the computed 2-loop potentials in 3d and in 4d [19].

To make this comparison simple two facts can be taken into account. First, we write the 4d analogue of the H-function as¹⁰ (sf. eq. (3.17) of ref.[19])

$$H^{4d}(m_1, m_2, m_3) = \frac{T^2}{(4\pi)^2} \left(\frac{1}{4\epsilon_B} + \frac{1}{4} l_\epsilon + \log \frac{3T}{\mu_3} + \bar{H}(m_1, m_2, m_3) + c \right), \quad (57)$$

where ϵ_B is given by (14), the constant l_ϵ is defined in eq. (3.13) of [19] (it cancels out in the final result). The numerical constant c is related to c_H computed numerically in [34]¹¹,

$$c \equiv \frac{1}{4}(2c_B - c_H) = -0.348725, \quad c_H = 5.3025, \quad c_B = \log(4\pi) - \gamma_E = 1.9538. \quad (58)$$

¹⁰The 4d sunset diagram can be decomposed as the sum of 3 pieces, $H^{4d} = H^{lll} + H_{hhh} + H_{hhl}$, where H_{hhh} is contribution containing only heavy 3d modes, H_{hhl} is a sum containing one light 3d mode and 2 heavy, while H^{lll} is 3d contribution defined in (32). In ref.[19] it was incorrectly asserted that H_{hhl} is suppressed by the light mass. The direct computation of H_{hhl} in the massless limit gives

$$H_{hhl} = -\frac{3}{64\pi^2} \left[\frac{1}{\epsilon} + 2(1 - \log 4 + \log \frac{\mu^2}{T^2}) \right]. \quad (56)$$

This mistake, as far as we can see, does not change the final results of ref.[19].

¹¹The constant c appears to be amazingly close to $-\frac{1}{2} \log 2$. However, we did not try to prove that this is indeed the case.

Second, we notice that if we choose the 4d scale parameter μ as in (15) then the constant c_B does not appear in any of the expressions defining high temperature asymptotic of the effective potential.

With this in mind consider first the simplest case, $O(N)$ scalar theory with $N=1$ discussed in the Section 5.2 with 4d lagrangian

$$\mathcal{L} = \frac{1}{2}(\partial_i\phi)^2 + \frac{1}{2}m^2\phi^2 + \frac{1}{4}\lambda\phi^4. \quad (59)$$

Comparing first the coefficients of the ϕ^4 terms in eq.(36) and in eq.(3.29) of [19] gives the result

$$\lambda_3 = [\lambda(\mu) + \frac{9}{16\pi^2}L_s\lambda^2]T = \lambda(\mu_T)T \quad (60)$$

in analogy with eq.(5) with μ_T defined in (15). Note that the last term arises from the term $-2c_B$ in L_s . To find out m_3^2 we compare the coefficients of the ϕ^2 term and express $\lambda(\mu_T)$ in terms of λ_3 . This gives the result

$$m_3^2(\mu_3) = \gamma(T^2 - T_0^2) + \frac{1}{16\pi^2} \left[-6\lambda_3^2 \left(\log \frac{3T}{\mu_3} + c \right) \right], \quad (61)$$

where

$$\gamma(T^2 - T_0^2) = \frac{1}{4}\lambda(\mu_T)T^2 - m^2(\mu_T). \quad (62)$$

Here the parameters $\lambda(\mu)$ and $m(\mu)$ are 4d quantities determined in the 4d theory by the coupling strength and the Higgs mass and by a choice of scale. In agreement with general relations, the coefficient of $\log(3T/\mu_3)$ is $f_{2m}/16\pi^2$ and the value of Λ_m in eq.(55) can be read from eq.(61). Note that the only μ_3 -dependent 3d quantity is the effective mass of the scalar particle, the 4d μ -dependence in the scalar self-coupling is cancelled out.

According to eq. (61) the choice of scale

$$\mu_3 = 3 \exp(c)T = 2.117T \quad (63)$$

makes the relation of $m_3^2(\mu_3)$ to 4d parameters be most simple.

The corresponding relations in the $SU(2)$ case are more complicated. Comparing with [19] we can now list the additional 4d contributions which have to be added to our 3d result for the various diagrams listed in Appendix B:

$$\begin{aligned} (d1) &= -\frac{7}{16}g_3^2m_T^2, \\ (d2) &= \frac{39}{16}g_3^2m_T^2, \\ (f2) &= \frac{1}{16}g_3^2(4m_T^2 + m_1^2 + 3m_2^2), \end{aligned} \quad (64)$$

All other diagrams give the same contribution in 3d and in high temperature limit of 4d.

There are also two counter term diagrams (wave function renormalization of the vector field and renormalization of the $\phi^\dagger\phi(A_i^a)^2$ vertex) without a 3d counterpart contributing $59g_3^2m_T^2/48$.

With this one can get ¹²

$$\begin{aligned}
m_3^2(\mu_3) &= \left[\frac{3}{16}g^2(\mu_T) + \frac{1}{2}\lambda(\mu_T) + \frac{g^2}{(4\pi)^2} \left(\frac{167}{96}g^2 + \frac{3}{4}\lambda \right) \right] T^2 \\
&\quad - \frac{1}{2}m^2(\mu_T) + \frac{1}{16\pi^2} \left[f_{2m} \left(\log \frac{3T}{\mu_3} + c \right) \right] = \\
&\quad \left[\frac{3}{16}g_3^2T + \frac{1}{2}\lambda_3T + \frac{g_3^2}{(4\pi)^2} \left(\frac{149}{96}g_3^2 + \frac{3}{4}\lambda_3 \right) \right] - \frac{1}{2}m_H^2 + \frac{1}{16\pi^2} \left[f_{2m} \left(\log \frac{3T}{\mu_3} + c \right) \right].
\end{aligned} \tag{66}$$

This relation is a central result of this Section.

7 Parameters of the EW phase transition from perturbation theory

7.1 The 2-loop results

Now, with effective field theories and the renormalization group at hand we are ready to present perturbative predictions for the critical temperature for the different Higgs masses. In our numerical estimates we used:

$$g_3^2 = \left(\frac{2}{3}\right)^2 T, \quad \lambda_3 = \frac{1}{8}g_3^2 \frac{m_H^2}{m_W^2}, \quad h_3 = \frac{1}{4}g_3^2, \quad \lambda_A = 0. \tag{67}$$

In other words, we have neglected 4d running of the couplings and masses. The parameter m_H is not the physical mass of the Higgs boson (defined by the pole of the scalar propagator) but the Lagrangian parameter in the \overline{MS} scheme at the normalization scale μ_T . As discussed in Section 2, the difference is quite small numerically.

The results are summarized in Table 1. The first 2 columns of the table provide the critical temperature and the expectation value of the Higgs field derived from the potential (49), in which $m_3^2(\mu)$ from eq.(66) is used. The next column is the value of the parameter κ for which the expectation value of the Higgs field at $T = T_c$ is the same for the 1-loop and 2-loop potentials. Pictures of typical potentials are presented in Fig.5 ($m_H = 35$ GeV) and Fig. 6 ($m_H = 80$ GeV). We stress that the deviation of the 1-loop RG improved potential from the 2-loop can be removed by change of the parameter μ .

¹²In order to escape confusion, we note that in ref. [19] the result for the effective potential is given in terms of 4d field normalized at scale T . This field is related to our 3d field as

$$\phi^2(T) = T\phi_3^2 \left(1 - \frac{9g^2}{32\pi^2} c_B \right). \tag{65}$$

m_H	T_c	ϕ_c	κ
35 GeV	93.2	160.7	2.03
60 GeV	140.3	96.6	1.91
70 GeV	157.5	87.3	1.83
80 GeV	173.3	81.0	1.75
90 GeV	187.9	76.1	1.66

Table 1: Numerical values of T_c and ϕ_c for various m_H values. The last column gives the value of κ in eq. (46) for which the 1- and 2-loop results coincide.

m_H	T_c	ϕ_c	κ
35 GeV	93.3	164.9	3.1
60 GeV	140.1	96.6	2.66
70 GeV	157.0	88.0	2.50
80 GeV	172.6	82.0	2.37
90 GeV	186.9	77.7	2.21

Table 2: As Table 1 but without the A_0 field.

In Table 2 we present the results for the theory where the heavy A_0 component has been integrated out. One can see that the difference is within 1 % for the critical temperature and ϕ_c . This proves that the A_0 field has small influence on the electroweak phase transition and indicates that higher order corrections associated with A_0 are numerically small.

7.2 Perturbative uncertainties in predictions

The crucial question with perturbative computations is of course whether they are reliable or not. As we discussed above, perturbation theory does not work at all at small scalar fields due to infrared divergences and a reliable estimate of the critical temperature is not possible. The effective potential has a logarithmic singularity at the origin at the 4-loop level and has the power divergent corrections at still higher loop levels. Just on dimensional grounds one can write the following expression for the effective potential coming from the loop expansion near the origin, starting from four loops:

$$V_{\geq 4}(\phi) = \frac{1}{2\pi} \left(\frac{g_3^2}{2\pi} \right)^3 \left(C_0 \log \frac{\mu_3}{m_T(\phi)} + \sum_{n=1}^{\infty} C_n \rho^n \right). \quad (68)$$

Due to the dimensionality of the gauge coupling constant the expansion parameter ρ is expected to be

$$\rho = \frac{1}{2\pi} \frac{g_3^2}{m_T(\phi)}, \quad (69)$$

where 2π comes from the loop integration, $m_T(\phi) = \frac{1}{2}g_3\phi$ and C_n are some numerical coefficients. This parameter is also the ratio of the typical terms of the 2- and 1-loop potentials calculated earlier. Perturbation theory explodes at $\phi = 0$ and is not applicable at $\rho > 1$. A natural way to estimate the uncertainties associated with the divergent behaviour of the perturbative expression for the effective potential near the origin is to *assume* that higher order corrections are not essential at $\rho < 1$ (i.e. at $m_T(\phi) > g_3^2/2\pi$) and to *assume* that they cannot change the value of the potential at the origin by more than $A/(2\pi)(g_3^2/2\pi)^3$ with $A \sim 1$ (cf. eq.(68)). Of course, these assumptions are completely ad hoc and cannot be proven by any perturbative methods. Moreover, as we will discuss in our paper [33], they are most probably wrong. Nevertheless, since our aim in this section is to estimate the *perturbative* uncertainties, we will make these assumptions. In any case, perturbative uncertainties are present and it is worthwhile to understand whether they are important numerically.

The explicit computation of the effective potential up to two loops, however, cannot help to estimate the convergence of perturbation theory. Quite an interesting situation arises. We cannot decide whether perturbation theory works well or not by comparing 1-loop and tree potentials, since just by chance the scalar self-interaction is smaller than the gauge one. At the same time, the comparison of the 1-loop result with the 2-loop one does not provide any information either, due to the μ -dependence (the 1-loop result is exactly equal to the 2-loop result with some particular choice of μ !).

This leads to the conclusion that most important uncertainties should come from the 3-loop corrections, since their contributions to the effective potential are parametrically larger than 4- and higher loop contributions. Unfortunately, the 3-loop computation is absent at present¹³, so that we can only guess what their magnitude can be. In what follows we consider two different types of corrections.

7.2.1 The renormalization group corrections

First of all, we know the μ -dependent logarithmic contribution on the 3-loop and even on the 4-loop level from the renormalization group. The 3-loop logarithmic correction to the effective potential is:

$$\begin{aligned} \Delta V_3 = & \frac{1}{16\pi^2} \frac{\partial V_1(\phi)}{\partial m_3^2} f_{2m} \log\left(\frac{\mu_3}{m_T(\phi)}\right) = \\ & -2\left(\frac{1}{4\pi}\right)^3 (m_1 + 3m_2) \left(\frac{81}{16}g_3^4 + 9\lambda_3 g_3^2 - 12\lambda_3^2\right) \log\left(\frac{\mu_3}{m_T(\phi)}\right), \end{aligned} \quad (70)$$

and the 4-loop logarithmic terms are

$$\Delta V_4 = \frac{1}{16\pi^2} \frac{\partial V_2(\phi)}{\partial m_3^2} f_{2m} \log\left(\frac{\mu_3}{m_T(\phi)}\right), \quad (71)$$

¹³The number of different 3-loop graphs is about 100. We thank S. Larin for a discussion of this point.

M_H	$T_c, \kappa = 0.6$	$\phi_c, \kappa = 0.6$	$T_c, \kappa = 6$	$\phi_c, \kappa = 6$
35 GeV	93.2	160.6	93.1	160.7
60 GeV	140.6	96.3	139.9	97.2
70 GeV	157.9	86.9	156.8	88.5
80 GeV	174.0	80.4	172.3	82.6
90 GeV	188.7	75.3	186.4	78.6

Table 3: Estimated effect of the 3-loop logarithmic correction to the perturbative values of T_c and ϕ_c . Here κ_0 is the value of κ given in Table 1.

where

$$\begin{aligned}
16\pi^2 \frac{\partial V_2(\phi)}{\partial m_3^2} = & \frac{-9 g_3^2}{16} + \frac{9 \lambda_3}{128} + \frac{3 g_3^2 m_1^2}{8 (4 m_T^2 + 6 m_T m_1 + 2 m_1^2)} + \frac{3 g_3^3 \phi}{32 m_1} + \\
& \frac{3 g_3^3 m_1 \phi}{8 (4 m_T^2 + 6 m_T m_1 + 2 m_1^2)} + \frac{3 \lambda_3 \phi^2}{8192 m_1^2} + \frac{3 g_3^4 \phi^2}{16 m_1 (2 m_T + m_1)} + \\
& \frac{3 g_3^4 \phi^2}{32 m_1 (2 m_L + m_1)} - \frac{3 g_3^4 \phi^2}{32 m_1 (2 m_T + 2 m_1)} + \\
& \frac{3 \lambda_3 \phi^2}{8192 m_1 (m_1 + 2 m_2)} + \frac{3 \lambda_3 \phi^2}{4096 m_2 (m_1 + 2 m_2)} - \\
& \frac{3 m_1^2 \log(\frac{3 \mu_3}{m_1})}{2 \phi^2} - \frac{3 g_3^2 \log(\frac{3 \mu_3}{m_T + m_1})}{4} + \\
& \frac{3 m_1^2 \log(\frac{3 \mu_3}{m_T + m_1})}{\phi^2} + \frac{3 g_3^2 \log(\frac{3 \mu_3}{2 m_T + m_1})}{4} - \\
& \frac{3 m_1^2 \log(\frac{3 \mu_3}{2 m_T + m_1})}{2 \phi^2} + \frac{3 g_3^2 \log(\frac{3 \mu_3}{m_T + m_1 + m_2})}{2} + \frac{3 g_3^2 \log(\frac{6 \mu_3}{2 m_T + 4 m_2})}{2}. \tag{72}
\end{aligned}$$

In spite of the fact that in some terms the square of the Higgs field appears in the denominator, this expression is perfectly regular for $\phi \rightarrow 0$. The calculation of still higher order logarithmic terms is not possible with the knowledge of the 1- and 2-loop expressions. Now, these expressions can be used for the estimation of a part of 3-loop corrections with a ‘sensible’ choice of $\mu_3 \sim m_T(\phi)$. In practice we just varied the parameter κ in eq.(49) from 0.6 to 6 (this is roughly factor $3^{(\pm 1)}$ deviation from the “optimal” value defined in Table 1. The results of these variations are shown in Table 3. One can see that the corrections are quite small.

7.2.2 The 3-loop linear term

The logarithmic corrections we have discussed are associated with the 2-loop renormalization of the Higgs mass. There will be a plenty of other contributions (and, most probably, more important numerically), related to the self-interaction of the gauge particles. Just on dimensional grounds the 3-loop contribution is linear in the Higgs field

M_H	T_c with $\beta = 20$	ϕ_c with $\beta = 20$
35 GeV	92.2	166.2
60 GeV	137.5	111.0
70 GeV	153.9	104.5
80 GeV	168.9	100.3
90 GeV	182.8	97.5

Table 4: Estimated effect of a 3-loop linear term.

and may be parametrized as

$$\Delta V_3 = \frac{\beta}{(4\pi)^3} g_3^4 m_T(\phi), \quad (73)$$

with β being some unknown number. To get an idea of how large it can be let us take the theory without the A_0 field (as we saw, the A_0 influence is quite small) and compare the 1-loop gauge contribution $v_1 \sim \frac{1}{2\pi} m_T^3$ with the leading 2-loop contribution $v_2 \sim \frac{1}{(4\pi)^2} \frac{51}{8} g_3^2 m_T^2(\phi)$, assuming that the log is of the order of 1. The expansion parameter ρ from here is $\rho \sim v_2/v_1 \sim g_3^2/(\pi m_T(\phi))$. So, one can guess that $v_3 \sim v_2\rho \sim v_2^2/v_1$, i.e. β can be as large as $51^2/(8 \cdot 16) \sim 20$. We understand, of course, that estimates of this type can never be trusted, but we cannot do anything better. A number of constraints on higher order terms can be derived from the analysis of lattice data [33]. We just note here that negative values of β are certainly excluded [33].

In table 4 we present the results of a computation of T_c and ϕ_c with the effective potential to which the linear term (73) is added. We vary the constant β from 0 to 20, positive values of β decrease the critical temperature and increase the expectation value, while the effect of a negative β is the opposite. As one can see, the uncertainty induced by this correction is considerably larger than from log type contributions but still within 20 % for the vacuum expectation value of the Higgs field at the critical temperature¹⁴. In order to avoid confusion, we also stress here that the upper bound on the Higgs mass, following from the requirement [4] $v/T > 1.5$ *cannot* be extracted from the perturbative effective potential at the perturbative critical temperature (as was done, e.g. in [18, 19, 21]) since the bubble nucleation temperature can be substantially lower than T_c [24].

8 Conclusions

We have considered the effective field theory approach to the study of the finite T electroweak phase transition. We have constructed explicitly an effective 3d SU(2) gauge field + fundamental Higgs + adjoint Higgs effective theory and studied its renormalization in detail. The main result is that the large logarithms found in refs. [18, 19] on the 2-loop level are in fact harmless and can be summed up in all orders of perturbation

¹⁴For negative $\beta \sim -20$ the correction is 100 % important.

theory by standard renormalization group methods applied to the 3d effective theory. We have further derived an effective theory by integrating away the heavy adjoint A_0 field .

Our results indicate that the 3d effective field theory approach is a very useful one for the perturbative study of hot electroweak matter in the broken phase. They form a necessary background for non-perturbative lattice Monte Carlo simulations of the system, which are required to clarify the properties of the phase transition and the symmetric phase.

A Appendix A

In this appendix we carry out the computation of the logarithmically divergent 2-loop counter term. The result could be obtained as a limit of the 2-loop potential, but a separate calculation is both illustrative and useful as a check.

The relevant Feynman diagrams were shown in Figs. 1-3. Landau gauge is used for A_i^a so that diagrams with a zero-momentum external scalar line emitting a single A_i^a line vanish, only the 4-vertex remains. For generality we give the results for $SU(N_c)$ gauge field coupled to a fundamental and adjoint Higgs. The relevant fundamental-adjoint couplings are then ($A_0 = A_0^a T^a$, $\text{Tr } T^a T^b = \frac{1}{2} \delta_{ab}$, $(T^a T^a)_{ij} = C_F \delta_{ij}$)

$$g_3^2 \phi^\dagger A_0 A_0 \phi, \quad g_3^2 \phi^\dagger A_i A_i \phi, \quad (74)$$

the adjoint-adjoint coupling is (A_0^a is an adjoint vector, $A_i = A_i^a F^a$, $\text{Tr } F^a F^b = N \delta_{ab}$)

$$\frac{1}{2} g_3^2 A_0 A_i A_i A_0, \quad (75)$$

and the scalar self-couplings are

$$\frac{1}{4} \lambda_3 (\phi_k \phi_k)^2, \quad \frac{1}{4} \lambda_A (A_0^a A_0^a)^2. \quad (76)$$

Consider first the 1-loop diagrams in Fig. 1. In the calculation of the 2-loop diagrams we shall actually need the 1-loop diagrams with an exact propagator $D(k) = 1/[k^2 + \Pi(k)]$, $D_{ij}(k) = (\delta_{ij} - k_i k_j / k^2) / [k^2 + \Pi_T(k)]$ in the loop. Using the above couplings to sum over all the contributing intermediate states one obtains the following contributions to δm^2 from the diagrams in Fig. 1:

$$\begin{aligned} \delta m_{(a)}^2 &= 2g_3^2 C_F \Sigma(\Pi_T(k)), \\ \delta m_{(b)}^2 &= g_3^2 C_F \Sigma(\Pi_0(k)), \\ \delta m_{(c)}^2 &= 2(N_c + 1) \lambda_3 \Sigma(\Pi_\phi(k)), \\ \delta m_{D(d)}^2 &= 2g_3^2 N_c \Sigma(\Pi_T(k)), \\ \delta m_{D(e)}^2 &= (N_c^2 + 1) \lambda_A \Sigma(\Pi_0(k)), \\ \delta m_{D(f)}^2 &= g_3^2 \Sigma(\Pi_\phi(k)), \end{aligned} \quad (77)$$

where we have abbreviated

$$\Sigma(\Pi(k)) = \int \frac{d^3k}{(2\pi)^3} \frac{1}{k^2 + \Pi(k)}. \quad (78)$$

For the 1-loop diagrams $\Pi(k) = 0$ and the counter terms in eq.(26) are obtained after taking $N_c = 2, C_F = 3/4$.

The 2-loop diagrams in Figs. 2-3 are of two different types, the sunset graphs (a)-(c) and the improved 1-loop graphs (d)-(h). Consider first their general structure neglecting the exchange and internal symmetry factors.

The sunset graphs come in two different variants, one with three scalars in the intermediate state, the other with two vectors and one scalar. The former is obviously proportional to

$$H_{\text{SSS}} \equiv H = \frac{1}{16\pi^2} \frac{1}{\epsilon}, \quad (79)$$

while for the latter (in Landau gauge) we find

$$H_{\text{SVV}} = \int \frac{d^3p}{(2\pi)^3} \frac{d^3q}{(2\pi)^3} \frac{1}{\mathbf{p}^2 \mathbf{q}^2 |\mathbf{p} + \mathbf{q}|^2} \left[1 + \frac{(\mathbf{p} \cdot \mathbf{q})^2}{\mathbf{p}^2 \mathbf{q}^2} \right] = \frac{3}{2} H. \quad (80)$$

The improved 1-loop graphs lead to a logarithmic divergence due to the fact that (already for dimensional reasons) the 1-loop self energy $\Pi(k)$ depends linearly on k in 3d: $\Pi(k) = \text{const} \times \text{coupling} \text{const.} \times k$. The linearly divergent piece of $\Pi(k)$ is removed by the mass counter term. Writing $\Pi(k) = Ak$ we have

$$\Sigma(\Pi(p)) = \int \frac{d^3p}{(2\pi)^3} \frac{1}{\mathbf{p}^2 + Ap} \approx \Sigma - A \int \frac{d^3p}{(2\pi)^3} \frac{1}{\mathbf{p}^3} = \Sigma - 8AH. \quad (81)$$

The calculation of the A_i propagator gives [26] -[27]

$$\Pi_T(k) = \frac{1}{64} [(11 - 2)N_c - 2] g_3^2 k, \quad (82)$$

where $11N_c$ comes from the A_i loop (11 is actually $10 + (1 + \xi)^2$ in an arbitrary covariant gauge), $-2N_c$ from the A_0 and -2 from the ϕ loop. For the A_0 and ϕ propagators

$$\Pi_0(k) = \frac{N_c}{4} g_3^2 k, \quad \Pi_\phi(k) = \frac{C_F}{4} g_3^2 k. \quad (83)$$

Calculating finally the symmetry factors of the sunset diagrams one obtains the following result for the various diagrams in Fig. 2 contributing to δm^2 ($C_F = (N_c^2 - 1)/(2N_c)$, $[T^a T^b (T^a T^b + T^b T^a)]_{ij} = (N_c^2 - 1)(N_c^2 - 2)/(4N_c^2) \delta_{ij}$):

$$\begin{aligned} (a) = \frac{3}{2}(b) &= -\frac{3(N_c^2 - 1)(N_c^2 - 2)}{8N_c^2} g_3^4 H, \\ (c) &= -4(N_c + 1) \lambda_3^2 H, \\ (d) + (e) + (f) &= \frac{1}{4} C_F (9N_c - 2) g_3^4 H, \\ (g) &= 2C_F N_c g_3^4 H, \\ (h) &= 4C_F (N_c + 1) \lambda_3 g_3^2 H, \end{aligned} \quad (84)$$

The sunset diagrams come with a $-$ sign from the expansion of $\exp(-\Gamma) \sim f \exp(-S)$. The final δm^2 is the sum of these; specializing to $N_c = 2$ one obtains the result in eq. (27).

Similarly, the diagrams in Fig. 3 contributing to δm_D^2 are (using $[F^c F^d (F^c F^d + F^d F^c)]_{ab} = \frac{3}{2} N_c^2 \delta_{ab}$, $\text{Tr} T^a T^c (T^c T^b + T^b T^c) = (N_c^2 - 2)/(4N_c) \delta_{ab}$):

$$\begin{aligned}
(a) &= -\frac{9}{4} N_c^2 H, \\
(b) &= -(N_c^2 + 1) \lambda_A^2 H, \\
(c) &= -\frac{N_c^2 - 2}{2N_c} g_3^4 H, \\
(d) + (e) + (f) &= \frac{1}{4} N_c (9N_c - 2) H, \\
(g) &= 2N_c (N_c^2 + 1) \lambda_A g_3^2 H, \\
(h) &= 2C_F g_3^4 H.
\end{aligned} \tag{85}$$

Now the sum (a)+(c)+(d)+(e)+(f)+(h)=0 and only the diagrams (b) and (g) containing the small induced coupling λ_A survive in the result eq.(27):

$$\delta m_D^2 = (N_c^2 + 1) \lambda_A (2N_c g_3^2 - \lambda_A). \tag{86}$$

B Appendix B

In this Appendix we carry out the computation of the 2-loop effective potential of the 3D effective theory defined by eq.(3). We give further the result obtained from this theory by integrating out the A_0 field as well as the results also for the U(1) Higgs model both with and without the A_0 field.

The relevant Feynman diagrams are shown in Fig.4, where the numbering relates to Fig. 2. The diagrams come in two different variants (see below), the sunset diagrams (a)-(c) and the closed figure-eight diagrams (d1)-(h4). The sunset diagrams are as in Fig. 2, the closed diagrams are obtained by adding to the bubble diagrams (d)-(h) also the corresponding diagrams with a 4-vertex. Thus one obtains the figure-eight diagrams in Fig. 4: they did not contribute to the logarithmic divergence but they do contribute to the potential.

Landau gauge and dimensional regularization with $d = 3 - 2\epsilon$ will be used throughout. The ϵ dependence is shown, if needed, only in connection of perturbative momentum space integrals.

B.1 The scalar O(N) theory

To show the technique [32] and to carry out the renormalization in some detail, consider first a 3d O(N) symmetric scalar model with Lagrangian ($a = 1, \dots, N$)

$$\mathcal{L} = \frac{1}{2} (\partial_i \phi_a)^2 + \frac{1}{2} m_0^2 \phi_a^2 + \frac{1}{4} \lambda (\phi_a^2)^2. \tag{87}$$

The dimensionalities of ϕ^2, λ, V are $\mu^{1-2\epsilon}, \mu^{1+2\epsilon}, \mu^{3-2\epsilon}$, respectively. As discussed earlier, there are only two divergent diagrams and one only has to introduce a mass counter term by writing $m_0^2 = m_R^2 + \delta m^2$, where m_R^2 is the renormalized mass. After shifting $\phi_1 \rightarrow \phi_0 + \phi_1$ and neglecting terms linear in ϕ_1 the Lagrangian becomes

$$\mathcal{L} = \frac{1}{2}m_0^2\phi_0^2 + \frac{1}{4}\lambda\phi_0^4 + \frac{1}{2}(\partial_i\phi_a)^2 + \frac{1}{2}m_1^2\phi_1^2 + \frac{1}{2}m_2^2(\phi_2^2 + \dots\phi_N^2) + \quad (88)$$

$$+ \lambda\phi_0\phi_1\phi_a^2 + \frac{1}{4}\lambda(\phi_a^2)^2 \equiv V_{\text{tree}}(\phi_0) + \mathcal{L}_0 + \mathcal{L}_1, \quad (89)$$

where $m_1^2 = m_0^2 + 3\lambda\phi_0^2$, $m_2^2 = m_0^2 + \lambda\phi_0^2$. The 2-loop effective potential is then calculated from the functional integral

$$\begin{aligned} \exp\left[-\frac{1}{\hbar}\mathcal{V}_3 V_{\text{eff}}(\phi_0)\right] &= \exp\left[-\frac{1}{\hbar}\mathcal{V}_3 V_{\text{tree}}(\phi_0)\right] \cdot \quad (90) \\ &\cdot \int \mathcal{D}\phi \exp\left[-\frac{1}{\hbar} \int d^3x \mathcal{L}_0\right] \left\langle \exp\left(-\frac{1}{\hbar} \int d^3x \mathcal{L}_1\right) \right\rangle, \end{aligned}$$

where \mathcal{V}_3 is the three-volume and where we have introduced a formal expansion parameter $1/\hbar$. Rescaling the variable of integration $\phi_a \rightarrow \phi_a \sqrt{\hbar}$ gives

$$\begin{aligned} V_{\text{eff}}(\phi_0) &= V_{\text{tree}}(\phi_0) - \frac{\hbar}{\mathcal{V}_3} \log \int \mathcal{D}\phi \exp\left[-\int d^3x \mathcal{L}_0\right] - \quad (91) \\ &- \frac{\hbar}{\mathcal{V}_3} \left\langle \exp\left[-\int d^3x (\lambda\phi_0\phi_1\phi_a^2\sqrt{\hbar} + \frac{1}{4}\lambda\phi_a^2\phi_b^2\hbar)\right] \right\rangle. \end{aligned}$$

In the course of the rescaling m_0^2 becomes $m_0^2 = m_R^2 + \hbar^2\delta m^2$; one \hbar comes from the expansion of $\exp[-\mathcal{L}_1]$, the other is the \hbar in front of the last term in eq.(91).

The Gaussian 1-loop integral is carried out in \mathbf{k} -space using

$$\mu^{2\epsilon} \int \frac{d^d k}{(2\pi)^d} \log(\mathbf{k}^2 + m^2) = -\frac{1}{6\pi} m^3 \quad (92)$$

with the result

$$V_{(1)}(\phi_0) = -\frac{\hbar}{12\pi} \mu^{-2\epsilon} [m_1^3 + (N-1)m_2^3]. \quad (93)$$

It is essential that we here can write $m_1^3 = [m_R^2 + \hbar^2\delta m^2 + 3\lambda\phi_0^2]^{3/2} = [m_R^2 + 3\lambda\phi_0^2]^{3/2} + \mathcal{O}(\hbar^2)$ so that the δm^2 term only gives an \hbar^3 correction to the potential, which to 2 loops is calculated to order \hbar^2 .

For the 2-loop contribution one first has to compute the expectation value of

$$-\int d^3x \mathcal{L}_1 = -\int d^3x \hbar \frac{1}{4} \lambda [\phi_1^2(x) + \dots + \phi_N^2(x)] [\phi_1^2(x) + \dots + \phi_N^2(x)]. \quad (94)$$

Each pairwise contraction gives (neglecting a common factor of \mathcal{V}_3)

$$I(m) = \mu^{-2\epsilon} \int \frac{d^d k}{(2\pi)^d} \frac{1}{\mathbf{k}^2 + m^2} = -\frac{m}{4\pi}. \quad (95)$$

There are four different types of contractions corresponding to the figure-eight diagram (h4). The first type is $\langle \phi_1 \phi_1 \phi_1 \phi_1 \rangle$, gives $3m_1^2/(4\pi)^2$ and appears only once. The second type $\langle \phi_2 \phi_2 \phi_2 \phi_2 \rangle$ appears $N-1$ times each giving $3m_2^2/(4\pi)^2$. The third type $\langle \phi_1 \phi_1 \phi_2 \phi_2 \rangle$ gives $m_1 m_2/(4\pi)^2$ and appears $2(N-1)$ times and the fourth type $\langle \phi_2 \phi_2 \phi_3 \phi_3 \rangle$ appears $(N-1)(N-2)$ times each giving $m_2^2/(4\pi)^2$. The total contribution to the potential from the scalar figure-eight diagram, taking into account the sign of V_{eff} in eq.(91), is

$$V_{(2)}^{(h4)}(\phi_0) = \frac{\lambda \mu^{-4\epsilon} \hbar^2}{64\pi^2} [3m_1^2 + 2(N-1)m_1 m_2 + (N^2-1)m_2^2]. \quad (96)$$

The second contribution to the 2-loop potential comes from the last term in eq. (91) and requires the calculation of the vacuum expectation value of

$$\frac{1}{2} \hbar \lambda^2 \int d^3 x \int d^3 y \phi_0 \phi_1(x) \phi_a(x) \phi_a(x) \cdot \phi_0 \phi_1(y) \phi_a(y) \phi_a(y). \quad (97)$$

This contains automatically the factor ϕ_0^2 and corresponds to the sunset diagram (c). There are two different types of contractions, $\langle \phi_1(x) \phi_1(x) \phi_1(x) \phi_1(y) \phi_1(y) \phi_1(y) \rangle$ appears once and gives $6H(m_1, m_1, m_1)$, where H is the dimensionless sunset function defined earlier, and $\langle \phi_1(x) \phi_2(x) \phi_2(x) \phi_1(y) \phi_2(y) \phi_2(y) \rangle$ appears $N-1$ times each giving $2H(m_1, m_2, m_2)$. The total contribution from the scalar sunset diagram is

$$V_{(2)}^{(c)}(\phi_0) = -\lambda^2 \mu^{-4\epsilon} \hbar^2 \phi_0^2 [3H(m_1, m_1, m_1) + (N-1)H(m_1, m_2, m_2)]. \quad (98)$$

Before renormalization the total 2-loop potential is the sum of V_{tree} and eqs.(93,96,98).

To carry out renormalization we insert $H(m_1, m_2, m_2) = [1/(4\epsilon) + \log[\mu/(m_1+2m_2)] + 1/2]/(16\pi^2)$ and find the following coefficient of the $\frac{1}{2}\phi_0^2$ term in the 2-loop potential:

$$m_R^2 + \hbar^2 \delta m^2 - \frac{6\lambda^2 \mu^{-4\epsilon} \hbar^2}{16\pi^2} \left(\frac{2+N}{3} \frac{1}{4\epsilon} + \log \frac{\mu}{3m_1} + \frac{N-1}{3} \log \frac{\mu}{m_1+2m_2} + \frac{N+2}{6} \right). \quad (99)$$

renormalization is carried out by choosing the counter term

$$\delta m^2 = \frac{2(2+N)\lambda^2 \mu^{-4\epsilon}}{16\pi^2} \frac{1}{4\epsilon}. \quad (100)$$

Since the bare mass term $m_R^2 + \hbar^2 \delta m^2$ has to be independent of μ , this counter term implies that

$$\mu \frac{\partial m_R^2}{\partial \mu} = -\frac{f_{2m}}{16\pi^2}, \quad f_{2m} = -2(N+2)\lambda^2. \quad (101)$$

The 2-loop potential in the final renormalized form then is

$$\begin{aligned} V_{\text{eff}}(\phi_0) &= \frac{1}{2} m_R^2(\mu) \phi_0^2 + \frac{1}{4} \lambda \phi_0^4 - \\ &- \frac{\hbar}{12\pi} [m_1^3 + (N-1)m_2^3] + \mathcal{O}(\hbar^3) + \\ &+ \frac{\lambda \hbar^2}{64\pi^2} [3m_1^2 + 2(N-1)m_1 m_2 + (N^2-1)m_2^2] - \\ &- 3 \frac{\lambda^2 \hbar^2}{16\pi^2} \left(\log \frac{\mu}{3m_1} + \frac{N-1}{3} \log \frac{\mu}{m_1+2m_2} + \frac{N+2}{6} \right) \phi_0^2 + \mathcal{O}(\hbar^4). \end{aligned} \quad (102)$$

where $m_1^2 = m_R^2(\mu) + 3\lambda\phi_0^2$, $m_2^2 = m_R^2(\mu) + \lambda\phi_0^2$. In view of eq.(101) one also explicitly has

$$\mu \frac{\partial V_{\text{eff}}(\phi_0)}{\partial \mu} = 0. \quad (103)$$

B.2 SU(2)-Higgs theory

The problem can be separated in two parts: computation of the momentum integrals with massive propagators and computation of the colour and symmetry factors. We shall mainly discuss the former.

There are three more difficult non-figure-eight diagrams in Fig.4: the vector loop-scalar (VVS) diagram (a), the scalar loop vector (SSV) diagrams (e1),(f1) and the vector loop-vector (VVV) diagram (d1). After performing the propagator contractions in the Landau gauge the VVS diagram is

$$(a) = D_{VVS}(M, M, m) = \int \frac{d^d p}{(2\pi)^d} \frac{d^d q}{(2\pi)^d} \frac{(1 - 2\epsilon)\mathbf{p}^2 \mathbf{q}^2 + (\mathbf{p} \cdot \mathbf{q})^2}{\mathbf{p}^2(\mathbf{p}^2 + M^2)\mathbf{q}^2(\mathbf{q}^2 + M^2)[(\mathbf{p} + \mathbf{q})^2 + m^2]}. \quad (104)$$

Here $d = 3 - 3\epsilon$. This diagram as well as the others are evaluated using the following:

1. Write for each combination

$$\frac{1}{\mathbf{p}^2(\mathbf{p}^2 + m^2)} = \frac{1}{m^2} \left(\frac{1}{\mathbf{p}^2} - \frac{1}{\mathbf{p}^2 + m^2} \right) \quad (105)$$

and split each integral as a sum of zero-mass and massive terms.

2. If the integrand is of the form $f(\mathbf{p}^2)g(\mathbf{q}^2)(\mathbf{p} \cdot \mathbf{q})^n$, the integral vanishes for n odd and one can replace

$$(\mathbf{p} \cdot \mathbf{q})^2 \rightarrow \frac{1}{d} \mathbf{p}^2 \mathbf{q}^2, \quad (\mathbf{p} \cdot \mathbf{q})^4 \rightarrow \frac{1}{d+2} \mathbf{p}^4 \mathbf{q}^4. \quad (106)$$

- d. Write $\mathbf{p} \cdot \mathbf{q} = \frac{1}{2}[(\mathbf{p} + \mathbf{q})^2 - \mathbf{p}^2 - \mathbf{q}^2]$ and add and subtract here mass terms so that you obtain same propagators as in the denominator.

4. Use that in dimensional regularization (n, m, l are integer positive powers)

$$\int \frac{d^d p}{(2\pi)^d} \frac{d^d q}{(2\pi)^d} \frac{\mathbf{p}^n \mathbf{q}^m (\mathbf{p} + \mathbf{q})^l}{\mathbf{p}^2 + m^2} = 0 \quad (107)$$

since the integral can be written as a sum of integrals from which one is scale-free and thus vanishing. Further

$$I(m_1, m_2) = \int \frac{d^d p}{(2\pi)^d} \frac{d^d q}{(2\pi)^d} \frac{1}{(\mathbf{p}^2 + m_1^2)(\mathbf{q}^2 + m_2^2)} = \frac{m_1 m_2}{16\pi^2}, \quad (108)$$

$$L(m_1, m_2) = \int \frac{d^d p}{(2\pi)^d} \frac{d^d q}{(2\pi)^d} \frac{(\mathbf{p} \cdot \mathbf{q})^2}{\mathbf{p}^2(\mathbf{p}^2 + m_1^2)\mathbf{q}^2(\mathbf{q}^2 + m_2^2)} = \frac{1}{3} \frac{m_1 m_2}{16\pi^2}, \quad (109)$$

and

$$\begin{aligned} \mu^{4\epsilon} \int \frac{d^d p}{(2\pi)^d} \frac{d^d k}{(2\pi)^d} \frac{1}{(\mathbf{p}^2 + m_1^2)(\mathbf{k}^2 + m_2^2)(|\mathbf{p} + \mathbf{k}|^2 + m_3^2)} &= \\ = H(m_1, m_2, m_3) &= \frac{1}{16\pi^2} \left(\frac{1}{4\epsilon} + \log \frac{\mu}{m_1 + m_2 + m_3} + \frac{1}{2} \right). \end{aligned} \quad (110)$$

The VVS diagram in eq.(104) then is, using rule 1.,

$$\begin{aligned} (a) = D_{VVS}(M, M, m) &= (1 - 2\epsilon)H(m, M, M) \\ &+ \frac{1}{M^4} [I(0, 0, m) - 2I(0, M, m) + I(M, M, m)], \end{aligned} \quad (111)$$

where

$$I(m_1, m_2, m_3) = \int \frac{d^d p}{(2\pi)^d} \frac{d^d q}{(2\pi)^d} \frac{(\mathbf{p} \cdot \mathbf{q})^2}{(\mathbf{p}^2 + m_1^2)(\mathbf{q}^2 + m_2^2)[(\mathbf{p} + \mathbf{q})^2 + m_3^2]}. \quad (112)$$

In view of eq. (110) the -2ϵ term here simply gives the constant $-1/2$. Calling the denominator in (112) $D_1 D_2 D_3$, $D_1 = \mathbf{p}^2 + m_1^2$, etc., the numerator, using rule 4., becomes $[D_3^2 + D_1^2 + D_2^2 + 2D_1 D_2 - 2D_2 D_3 - 2D_1 D_3 - 2(m_3^2 - m_2^2 - m_1^2)(D_3 - D_2 - D_1) + (m_3^2 - m_2^2 - m_1^2)^2]/4$. One obtains known integrals and

$$\int \frac{d^d p}{(2\pi)^d} \frac{d^d q}{(2\pi)^d} \frac{D_3}{D_1 D_2} = (m_3^2 - m_2^2 - m_1^2) m_1 m_2 \quad (113)$$

and permutations thereof. The sum is

$$\begin{aligned} I(m_1, m_2, m_3) &= \frac{1}{4} \left[(m_3^2 - m_2^2 - m_1^2)^2 H(m_1, m_2, m_3) + \right. \\ &+ 2(m_3^2 - m_2^2 - m_1^2) m_3 (m_1 + m_2) - \\ &- (m_3^2 - m_2^2 - m_1^2) m_1 m_2 + (m_1^2 - m_2^2 - m_3^2) m_3 m_2 + \\ &\left. + (m_2^2 - m_1^2 - m_3^2) m_3 m_1 \right], \end{aligned} \quad (114)$$

which leads to the final expression for the momentum integral for diagram (a):

$$\begin{aligned} (a) = D_{VVS}(M, M, m) &= \left\{ 2H(M, M, m) - \frac{1}{2}H(M, m, 0) + \right. \\ &+ \frac{m^2}{M^2} [H(M, m, 0) - H(M, M, m)] + \\ &+ \frac{m^4}{4M^4} [H(m, 0, 0) + H(M, M, m) - 2H(M, m, 0)] - \\ &\left. - \frac{m}{2M} - \frac{m^2}{4M^2} \right\} \end{aligned} \quad (115)$$

The second more complicated diagram is the scalar loop-vector diagram (SSV):

$$(e1), (f1) = D_{SSV}(m_1, m_2, M) = \int \frac{d^d p}{(2\pi)^d} \frac{d^d q}{(2\pi)^d} \frac{4[\mathbf{p}^2 \mathbf{q}^2 - (\mathbf{p} \cdot \mathbf{q})^2]}{(\mathbf{p}^2 + m_1^2) \mathbf{q}^2 (\mathbf{q}^2 + m_V^2) [(\mathbf{p} + \mathbf{q})^2 + m_2^2]}. \quad (116)$$

This equals

$$D_{SSV}(m_1, m_2, M) = \int \frac{d^d p}{(2\pi)^d} \frac{d^d q}{(2\pi)^d} \left[\frac{4}{D_2 D_3} - \frac{4m_1^2}{D_1 D_2 D_3} \right] - \frac{4}{M^2} [I(m_1, 0, m_2) - I(m_1, M, m_2)] \quad (117)$$

and one can directly use the integral in eq.(114) with the result

$$\begin{aligned} D_{SSV}(m_1, m_2, M) &= (M^2 - 2m_1^2 - 2m_2^2)H(M, m_1, m_2) + \\ &+ \frac{(m_1^2 - m_2^2)^2}{M^2} [H(M, m_1, m_2) - H(0, m_1, m_2)] + \\ &+ \frac{1}{M} \{ (m_1 + m_2)[M^2 + (m_1 - m_2)^2] - Mm_1 m_2 \}. \end{aligned} \quad (118)$$

The most complicated diagram is the vector loop-vector diagram (VVV):

$$\begin{aligned} (d1) &= D_{VVV}(m, m, m) = \\ &\int \frac{d^d p}{(2\pi)^d} \frac{d^d q}{(2\pi)^d} \frac{[(\mathbf{p} \cdot \mathbf{q})^2 - \mathbf{p}^2 \mathbf{q}^2][2\mathbf{p}^4 + 4\mathbf{p}^2 \mathbf{p} \cdot \mathbf{q} + (\mathbf{p} \cdot \mathbf{q})^2 + 5\mathbf{p}^2 \mathbf{q}^2 + 4\mathbf{p} \cdot \mathbf{q} \mathbf{q}^2 + 2\mathbf{q}^4]}{\mathbf{p}^2(\mathbf{p}^2 + m^2)\mathbf{q}^2(\mathbf{q}^2 + m^2)(\mathbf{p} + \mathbf{q})^2[(\mathbf{p} + \mathbf{q})^2 + m^2]} \\ &- 2\epsilon \int \frac{d^d p}{(2\pi)^d} \frac{d^d q}{(2\pi)^d} \frac{[(\mathbf{p} \cdot \mathbf{q})^2 - \mathbf{p}^2 \mathbf{q}^2][\mathbf{p}^4 + \mathbf{q}^4 + 2(\mathbf{p}^2 + \mathbf{q}^2)\mathbf{p} \cdot \mathbf{q} + d\mathbf{p}^2 \mathbf{q}^2]}{\mathbf{p}^2(\mathbf{p}^2 + m^2)\mathbf{q}^2(\mathbf{q}^2 + m^2)(\mathbf{p} + \mathbf{q})^2[(\mathbf{p} + \mathbf{q})^2 + m^2]}. \end{aligned} \quad (119)$$

Denoting the integral without the $\mathbf{p}^2, \mathbf{q}^2$ and $(\mathbf{p} + \mathbf{q})^2$ factors in the denominator by (m, m, m) , one obtains, by using eq.(105)

$$D_{VVV}(m, m, m) = -\frac{1}{m^6} \left[(m, m, m) - 3(m, m, 0) + 3(m, 0, 0) - (0, 0, 0) \right]. \quad (120)$$

The reduction techniques explained earlier lead to

$$\begin{aligned} (m, m, m) &= -\frac{63}{16}m^8 H(m, m, m) + \frac{183}{16}m^8 + \frac{9}{8}m^8, \\ (m, m, 0) &= \frac{10}{3}m^8, \\ (m, 0, 0) &= \frac{1}{16}m^8 H(m, 0, 0), \end{aligned} \quad (121)$$

where the last term in (m, m, m) arises from the -2ϵ term in (119). Adding up gives

$$D_{VVV}(m, m, m) = m^2 \left[\frac{63}{16}H(m, m, m) - \frac{3}{16}H(m, 0, 0) - \frac{41}{16} \right]. \quad (122)$$

The figure-eight diagrams lead to integrals of the type in eqs.(108-109) and are easy to evaluate. Including the charge and symmetry factors leads to the final result for the diagrams ($\times 16\pi^2$) in Fig.4:

$$(a) = -\frac{3}{16}g_3^4 \phi^2 \left\{ 2H(m_1, m_T, m_T) - \frac{1}{2}H(m_1, m_T, 0) + \right.$$

$$\begin{aligned}
& + \frac{m_1^2}{m_T^2} [H(m_1, m_T, 0) - H(m_1, m_T, m_T)] + \\
& + \frac{m_1^4}{4m_T^4} [H(m_1, 0, 0) + H(m_1, m_T, m_T) - 2H(m_1, m_T, 0)] - \\
& - \left. \frac{m_1}{2m_T} - \frac{m_1^2}{4m_T^2} \right\}, \tag{123}
\end{aligned}$$

$$(b) = -\frac{3}{16} g_3^4 \phi^2 H(m_1, m_L, m_L), \tag{124}$$

$$(c) = -3\lambda_3^2 \phi^2 [H(m_1, m_1, m_1) + H(m_1, m_2, m_2)], \tag{125}$$

$$(d1) = 2g_3^2 \left[\frac{63}{16} m_T^2 H(m_T, m_T, m_T) - \frac{3}{16} m_T^2 H(m_T, 0, 0) - \frac{41}{16} m_T^2 \right], \tag{126}$$

$$(\text{ghost}) = 2g_3^2 \frac{3}{8} m_T^2 H(m_T, 0, 0), \tag{127}$$

$$(d2) = 4g_3^2 m_T^2, \tag{128}$$

$$(e1) = -\frac{3}{2} g_3^2 [(m_T^2 - 4m_L^2) H(m_T, m_L, m_L) + 2m_T m_L - m_L^2], \tag{129}$$

$$(e2) = 6g_3^2 m_T m_L, \tag{130}$$

$$\begin{aligned}
(f1) = & -\frac{3}{8} g_3^2 \left[(m_T^2 - 2m_1^2 - 2m_2^2) H(m_1, m_2, m_T) + (m_T^2 - 4m_2^2) H(m_2, m_2, m_T) + \right. \\
& + \frac{(m_1^2 - m_2^2)^2}{m_T^2} [H(m_1, m_2, m_T) - H(m_1, m_2, 0)] + \\
& \left. + \frac{(m_1^2 - m_2^2)(m_1 - m_2)}{m_T} + m_T(m_1 + 3m_2) - m_1 m_2 - m_2^2 \right], \tag{131}
\end{aligned}$$

$$(f2) = \frac{3}{4} g_3^2 m_T (m_1 + 3m_2), \tag{132}$$

$$(g3) = \frac{15}{4} \lambda_A m_L^2, \tag{133}$$

$$(g4) = \frac{3}{8} g_3^2 m_L (m_1 + 3m_2), \tag{134}$$

$$(h4) = \frac{3}{4} \lambda_3 (m_1^2 + 2m_1 m_2 + 5m_2^2). \tag{135}$$

It may also be useful to quote the sum of all the non-Abelian diagrams

$$\begin{aligned}
& (d1) + (\text{ghost}) + (d2) + (e1) + (e2) = \\
& = g_3^2 m_T^2 \left[\frac{63}{8} H(m_T, m_T, m_T) + \frac{9}{2} H(m_T, m_L, m_L) + \frac{3}{8} H(m_T, 0, 0) + \frac{3}{8} \right] + \\
& + 3g_3^2 m_L m_T + 6g_3^2 m_3^2 H(m_T, m_L, m_L). \tag{136}
\end{aligned}$$

B.3 U(1)-Higgs theory

In this appendix we consider 4d U(1) Higgs theory defined by Lagrangian

$$L = \frac{1}{4} F_{\mu\nu} F_{\mu\nu} + (D_\mu \phi)^\dagger (D_\mu \phi) - \frac{1}{2} m^2 \phi^\dagger \phi + \lambda (\phi^\dagger \phi)^2. \tag{137}$$

The dimensionally reduced theory is

$$S_{\text{eff}}[A_i(\mathbf{x}), A_0(\mathbf{x}), \phi(\mathbf{x})] = \int d^3x \left\{ \frac{1}{4} F_{ij} F_{ij} + \frac{1}{2} (D_i A_0)(D_i A_0) + (D_i \phi)^\dagger (D_i \phi) + \frac{1}{2} m_D^2 A_0 A_0 + \frac{1}{4} \lambda_A (A_0 A_0)^2 + m_3^2 \phi^\dagger \phi + \lambda_3 (\phi^\dagger \phi)^2 + h_3 A_0^a A_0^a \phi^\dagger \phi \right\}. \quad (138)$$

The one-loop relations between 3d and 4d couplings and fields in the Landau gauge are:

$$g_3^2 = g^2(\mu) T \left[1 - \frac{g^2 L_s}{3(4\pi)^2} \right], \quad (139)$$

$$\lambda_3 = T \left[\lambda(\mu) - \frac{L_s}{(4\pi)^2} (3g^4 - 6\lambda g^2 + 10\lambda^2) + \frac{2}{(4\pi)^2} g^4 \right], \quad (140)$$

$$h_3 = g^2(\mu) T \left[1 - \frac{g^2 L_s}{3(4\pi)^2} + \frac{4g^2}{3(4\pi)^2} + \frac{8\lambda}{(4\pi)^2} \right] = \quad (141)$$

$$\frac{1}{4} g_3^2 \left[1 + \frac{4g^2}{3(4\pi)^2} + \frac{8\lambda}{(4\pi)^2} \right],$$

$$\lambda_A = \frac{g^4(\mu) T}{24\pi^2}, \quad (142)$$

$$m_D^2 = \frac{1}{3} g^2(\mu) T^2, \quad (143)$$

$$m_3^2 = \left[\frac{1}{4} g^2(\mu) + \frac{1}{3} \lambda(\mu) \right] T^2 - \frac{1}{2} m^2(\mu) \left[1 + \frac{L_s}{(4\pi)^2} (-3g^2 + 4\lambda) \right], \quad (144)$$

$$\phi^{3d} = \frac{1}{\sqrt{T}} \phi \left(1 - \frac{3g^2}{2(4\pi)^2} \frac{1}{\epsilon_B} \right), \quad (145)$$

$$A_0^{3d} = \frac{1}{\sqrt{T}} A_0 \left[1 + \frac{g^2}{6(4\pi)^2} \left(\frac{1}{\epsilon_B} + 2 \right) \right], \quad (146)$$

$$A_i^{3d} = \frac{1}{\sqrt{T}} A_i \left[1 + \frac{g^2}{6(4\pi)^2} \frac{1}{\epsilon_B} \right]. \quad (147)$$

As in the main body of the paper, we present the 2-loop potential with the use of simplified relations between couplings, namely

$$h_3 = g_3^2, \quad \lambda_A = 0 \quad (148)$$

The field dependent masses are:

$$m_T = g_3 \phi, \quad m_L^2 = m_D^2 + m_T^2 = \frac{1}{3} g^2 T^2 + m_T^2, \quad (149)$$

$$m_1^2 = m_3^2(\mu_3) + 3\lambda_3 \phi^2, \quad m_2^2 = m_3^2(\mu_3) + \lambda_3 \phi^2.$$

The 1-loop potential in 3d is

$$V(\phi) = \frac{1}{2}m_3^2(\mu_3) + \frac{1}{4}\lambda_3\phi^4 - \frac{T}{12\pi}(2m_T^3 + m_L^3 + m_1^3 + m_2^3). \quad (150)$$

In the calculation of the 2-loop potential in 3d the main difference with respect to SU(2) is that the non-Abelian diagrams in eq. (136) do not appear. Secondly, since there is only one Higgs and one Goldstone mode, the diagrams with two different Goldstone modes are missing. The color factors clearly also are different. The final result for the diagrams ($\times 16\pi^2$ for non- H diagrams) is

$$\begin{aligned} (a) &= -g^4\phi^2 D_{VVS}(m_1, m_T, m_T), \\ (b) &= -g^4\phi^2 H(m_1, m_L, m_L), \\ (c) &= -\lambda^2\phi^2[3H(m_1, m_1, m_1) + H(m_1, m_2, m_2)], \\ (f1) &= -\frac{1}{2}g^2 D_{SSV}(m_1, m_2, m_T), \\ (f2) + (g4) &= \frac{1}{2}g^2(m_L + 2m_T)(m_1 + m_2), \\ (h4) &= \frac{1}{4}\lambda(3m_1^2 + 2m_1m_2 + 3m_2^2). \end{aligned} \quad (151)$$

Again the coefficient of $\frac{1}{2}\phi^2 \log(\mu_3)$ in the sum gives the value of $f_{2m}/16\pi^2$ in the 3d running of the scalar mass $m_3^2(\mu_3)$,

$$m_3^2(\mu_3) = \frac{f_{2m}}{16\pi^2} \log \frac{\Lambda_m}{\mu_3}, \quad (152)$$

where

$$f_{2m} = -6g_3^4 + 8\lambda_3g_3^2 - 8\lambda_3^2 = -6g_3^4 \left(1 - \frac{2m_H^2}{3m_W^2} + \frac{m_H^4}{3m_W^4}\right) < 0. \quad (153)$$

with $\lambda_3 = g_3^2 m_H^2 / (2m_W^2)$. The relation between the temperature and the renormalization invariant scale Λ_m can be found as has been described in the Section. 6.

B.4 SU(2)-Higgs theory integrated over A_0

In view of the large value of m_D one may further simplify the effective theory by entirely integrating out the A_0 field, the effective action then becomes $S_{\text{eff}}[A_i^a, \phi_k]$. The integration can be carried out explicitly, but it is rather illuminating to derive the result by taking the large m_D limit of the 2-loop effective potential.

The relevant diagrams in eqs. (123-135) are those containing $m_L = \sqrt{m_D^2 + m_T^2}$. Expanding them to order $1/m_D$ and neglecting a constant term $\sim m_D^2[\log(\mu/2m_D) + 1/4]$ one obtains for the relevant diagrams (in evident notation)

$$\begin{aligned} (A_0A_0\phi) &= -\frac{3}{16}g^4\phi^2 \left(\log \frac{\mu}{2m_D} + \frac{1}{2}\right) + \frac{3}{8}g^2m_T^2 \frac{m_1}{m_D} + \dots, \\ (A_0A_0A_i) + (A_0A_i) &= \frac{9}{2}g^2m_T^2 \left(\log \frac{\mu}{2m_D} + \frac{1}{2}\right) - \frac{3}{4}g^2m_T^2 + \frac{g^2}{2m_D}m_T^3 + \dots, \\ (A_0\phi) &= \frac{3}{8}g^2m_D(m_1 + 3m_2) + \frac{3}{16}g^2m_T^2 \frac{m_1 + 3m_2}{m_D} + \dots \end{aligned} \quad (154)$$

Expanding also

$$m_L^3 = m_D^3 + \frac{3}{2}m_D m_T^2 + \frac{3}{8} \frac{m_T^4}{m_D} + \dots \quad (155)$$

gives the limit of the 2-loop potential as

$$\begin{aligned} V(m_D \gg g^2) &= \frac{1}{2} \left[m^2(\mu) - \frac{3g^2 m_D}{16\pi} + \frac{15}{(16\pi)^2} g^4 \left(\log \frac{\mu}{2m_D} + \frac{1}{2} \right) - \frac{3g^4}{128\pi^2} \right] \phi^2 \\ &+ \frac{1}{4} \left(\lambda - \frac{3g^4}{128\pi m_D} \right) \phi^4 - \frac{1}{12\pi} [6m_T^3 + m_1^3 + 3m_2^3] + \\ &+ \frac{g^2}{32\pi^2 m_D} m_T^3 + \frac{3}{128\pi^2} g^2 m_D (m_1 + 3m_2) + \frac{9g^2}{256\pi^2 m_D} m_T^2 (m_1 + m_2) + \\ &+ 2 - \text{loop diagrams in eqs. (123 - 135) without } A_0. \end{aligned} \quad (156)$$

If we now introduce new parameters by the following equations

$$\begin{aligned} \bar{m}_3^2(\mu_3) &= m_3^2(\mu_3) - \frac{3g_3^2 m_D}{16\pi} + \frac{30}{(16\pi)^2} g_3^4 \left(\log \frac{\mu_3}{2m_D} + \frac{3}{10} \right), \\ \bar{g}_3^2 &= g_3^2 \left(1 - \frac{g_3^2}{24\pi m_D} \right), \\ \bar{\lambda}_3 &= \lambda_3 - \frac{3g_3^4}{128\pi m_D}, \end{aligned} \quad (157)$$

we see that the m_D -dependent terms in eq. (156) are entirely cancelled. This is obviously so for the ϕ^2 and ϕ^4 terms. The transformation of g^2 combines the $m_T^3 = g^3 \phi^3/8$ terms and inserting the transformation of $m^2(\mu)$ and λ in $m_1^3 + 3m_2^3$ cancels the two last terms in eq. (156). The $g^4 \log(\mu/2m_D)$ term simply removes the A_0 loop contributions from f_{2m} and is otherwise of higher order—as is also the last term in the transformation of $m_3^2(\mu_3)$.

The effective potential of the effective theory obtained by integrating over A_0 is thus

$$\begin{aligned} V_{\text{eff}} &= \frac{1}{2} \bar{m}_3^2(\mu_3) \phi^2 + \frac{1}{4} \bar{\lambda}_3 \phi^4 - \frac{1}{12\pi} [6\bar{m}_T^3 + \bar{m}_1^3 + 3\bar{m}_2^3] + \\ &+ 2 - \text{loop diagrams in eqs. (123 - 135) without } A_0, \end{aligned} \quad (158)$$

where $\bar{m}_T = \frac{1}{2} \bar{g}_3 \phi$, $\bar{m}_1^2 = \bar{m}_3^2(\mu_3) + 3\bar{\lambda}_3 \phi^2$ and $\bar{m}_2^2 = \bar{m}_3^2(\mu) + \bar{\lambda}_3 \phi^2$. It is formally irrelevant whether one uses g_3 or \bar{g}_3 in the 2-loop diagrams; the difference is of higher order.

A direct diagrammatic derivation of eqs.(157) is straightforward: the first requires the evaluation of the A_0 1-loop and 2-loop contribution to the ϕ propagator, second the evaluation of the k^2 term in the A_0 loop contribution to the A_i propagator and the last the A_0 loop contribution to the self-coupling.

B.5 U(1)-Higgs theory integrated over A_0

The effective potential of the theory obtained from the U(1) theory after integrating out the A_0 field is

$$\begin{aligned}
V_{\text{eff}} = & \frac{1}{2}\bar{m}^2(\mu)\phi^2 + \frac{1}{4}\bar{\lambda}\phi^4 - \frac{1}{12\pi}[2\bar{m}_T^3 + \bar{m}_1^3 + \bar{m}_2^3] + \\
& + \frac{1}{16\pi^2}\left\{-g^4\phi^2 D_{VVS}(m_1, m_T, m_T) - \frac{1}{2}g^2 D_{SSV}(m_1, m_2, m_T)\right. \\
& - \lambda^2\phi^2[3\bar{H}(m_1, m_1, m_1) + \bar{H}(m_1, m_2, m_2)] + \\
& \left. + g^2 m_T(m_1 + m_2) + \frac{1}{4}(3m_1^2 + 2m_1 m_2 + 3m_2^2)\right\}, \tag{159}
\end{aligned}$$

where the couplings are related to those of the original theory by

$$\begin{aligned}
\bar{m}_3^2(\mu_3) &= m_3^2(\mu_3) - \frac{g_3^2 m_D}{4\pi} - \frac{1}{8\pi^2}g_3^4\left(\log\frac{\mu_3}{2m_D} + \frac{1}{2}\right), \\
\bar{\lambda}_3 &= \lambda_3 - \frac{g_3^4}{8\pi m_D}. \tag{160}
\end{aligned}$$

Due to the absence of non-Abelian coupling there is no rescaling of g_3^2 .

References

- [1] D. A. Kirzhnits, JETP Lett. 15 (1972) 529;
D. A. Kirzhnits and A. D. Linde, Phys. Lett. 72B (1972) 471.
- [2] A. Guth, Phys. Rev. D23 (1981) 347;
A.D. Linde, Phys. Lett. 108B (1982) 389;
A. Albrecht and P. Steinhardt, Phys. Rev. Lett. 48 (1982) 1220.
- [3] V. A. Kuzmin, V. A. Rubakov, and M. E. Shaposhnikov, Phys. Lett., 155B(1985)36.
- [4] M. E. Shaposhnikov. Nucl. Phys. B287 (1987) 757.
- [5] A.D. Linde, Phys. Lett. 96B (1980) 289.
- [6] D. Gross, R. Pisarski and L. Yaffe, Rev. Mod. Phys. 53 (1981) 43.
- [7] M. Reuter and C. Wetterich, Nucl. Phys. B408 (1993) 91.
- [8] D.A. Kirzhnits and A.D. Linde, Ann. Phys. 101 (1976) 195;
A.D. Linde, Nucl. Phys. B216 (1983) 421, Rep. Prog. Phys. 47 (1984)925.
- [9] G.W. Anderson and L.J. Hall, Phys. Rev. D45 (1992) 2685.
- [10] M. Carrington, Phys. Rev. D45 (1992) 2933.

- [11] M. Dine, R. Leigh, P. Huet, A. Linde and D. Linde, Phys. Rev. D46 (1992) 550.
- [12] C. G. Boyd, D. E. Brahm and S. Hsu, Phys. Rev. D48 (1993) 4963.
- [13] M. Quiros, J.R. Espinosa and F. Zwirner, Phys. Lett. B314 (1993) 206.
- [14] W. Buchmüller, T. Helbig and D. Walliser, Nucl. Phys. B407 (1993) 387.
- [15] G. Amelino-Camelia, Preprint BUHEP-93-12 (1993).
- [16] J. March-Russell, Phys.Lett. B296 (1992) 364.
- [17] W. Buchmüller, Z. Fodor, T. Helbig and D. Walliser, DESY Preprint DESY-93-021 (1993), Ann. Phys., to be published.
- [18] J. E. Bagnasco and M. Dine, Phys. Lett. B303 (1993) 308.
- [19] P. Arnold and O. Espinosa, Phys. Rev. D47 (1993) 3546.
- [20] A. Hebecker, Z. Phys. C60 (1993) 271.
- [21] P. Arnold and L. Yaffe, Preprint UW/PT-93-24 (1993).
- [22] B. Bunk, E.-M. Ilgenfritz, J. Kripfganz, A. Schiller, Phys. Lett. B284 (1992) 371; Nucl. Phys. B403 (1993) 453.
- [23] K. Kajantie, K. Rummukainen and M. Shaposhnikov, Nucl. Phys. B407 (1993) 356.
- [24] M. Shaposhnikov, Phys. Lett. B316 (1993) 112.
- [25] S. Weinberg, Phys. Lett. 91B (1980) 51.
- [26] T. Appelquist and R. Pisarski, Phys. Rev. D23 (1981) 2305.
- [27] S. Nadkarni, Phys. Rev. D27 (1983) 917.
- [28] N. P. Landsman, Nucl. Phys. B322 (1989) 498.
- [29] P. Lacock, D. E. Miller and T. Reisz, Nucl. Phys. B369 (1992) 501.
- [30] L. Kärkkäinen, P. Lacock, B. Petersson and T. Reisz, Nucl. Phys. B395 (1993) 733.
- [31] A. Jakovác, K. Kajantie and A. Patkós, Helsinki Preprint HU-TFT-94-01, hep-ph-9312355.
- [32] R. Jackiw, Phys. Rev. D9 (1974) 1686.
- [33] K. Farakos, K. Kajantie, K. Rummukainen and M. Shaposhnikov, in preparation.
- [34] R. Parwani, Phys. Rev. D45 (1992) 4695.

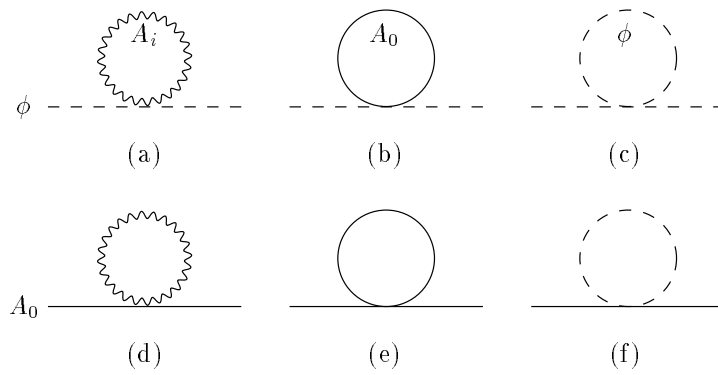


Figure 1: The one-loop linear-divergent diagrams contributing to the mass of the doublet and the triplet of scalar fields.

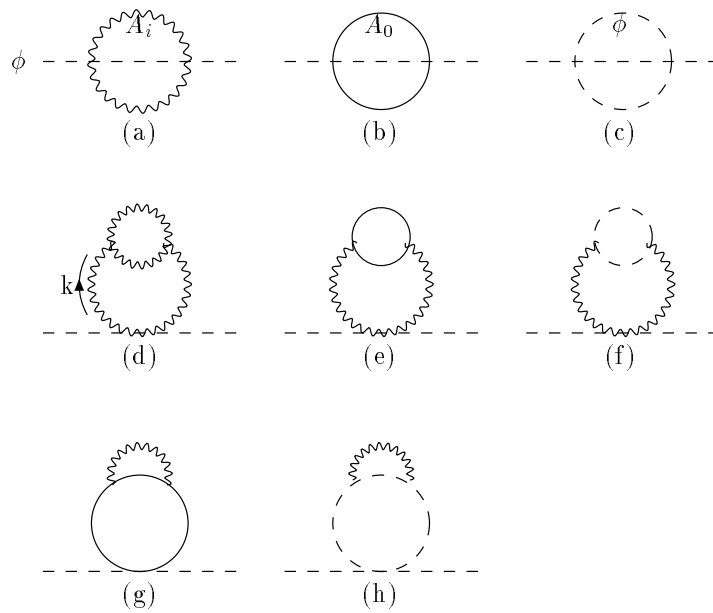


Figure 2: The two-loop log-divergent diagrams contributing to the mass of the doublet of scalar fields.

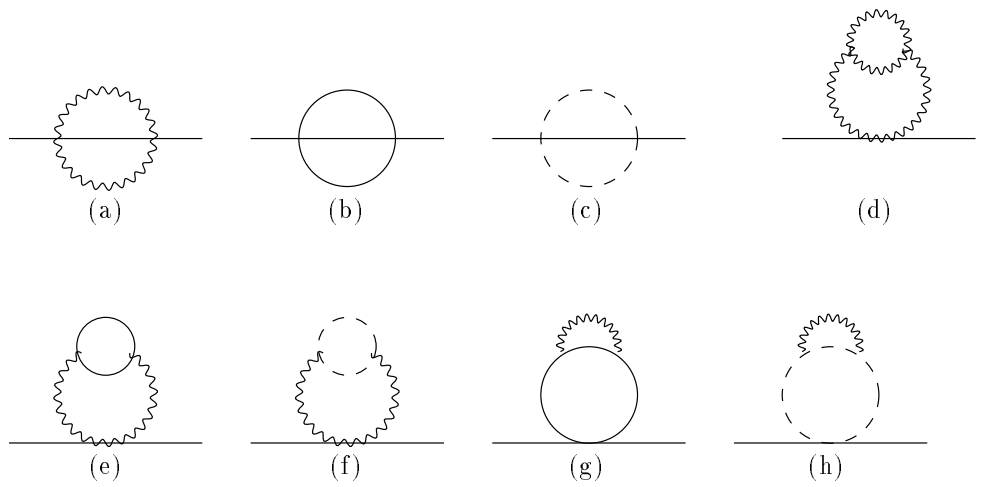


Figure 3: The two-loop log-divergent diagrams contributing to the mass of the triplet of scalar fields.

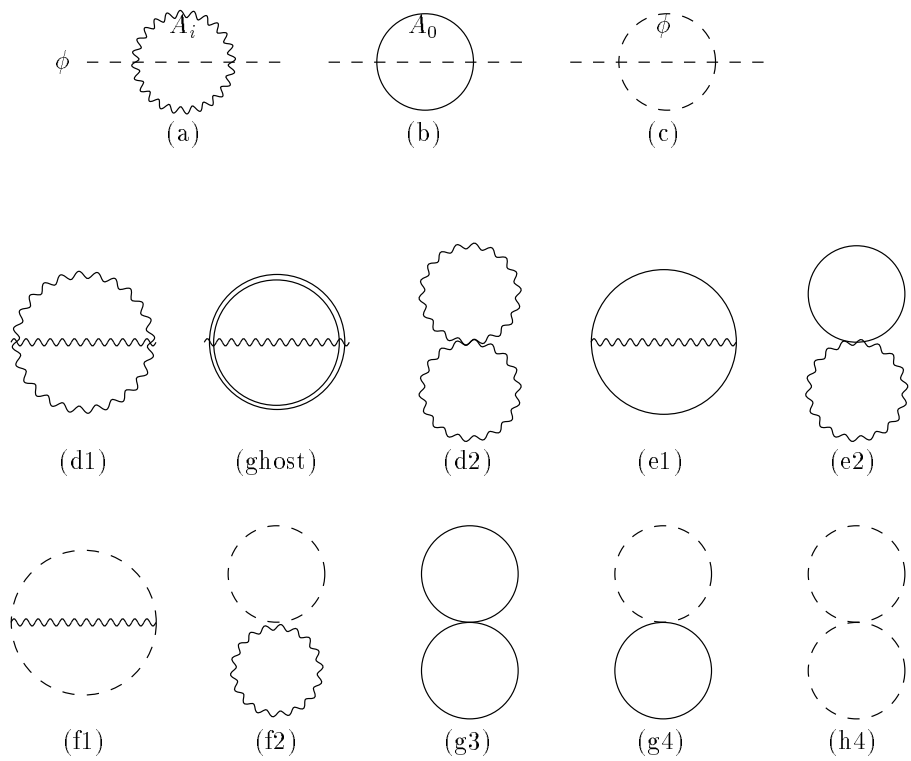


Figure 4: The two-loop contributions to the effective potential.

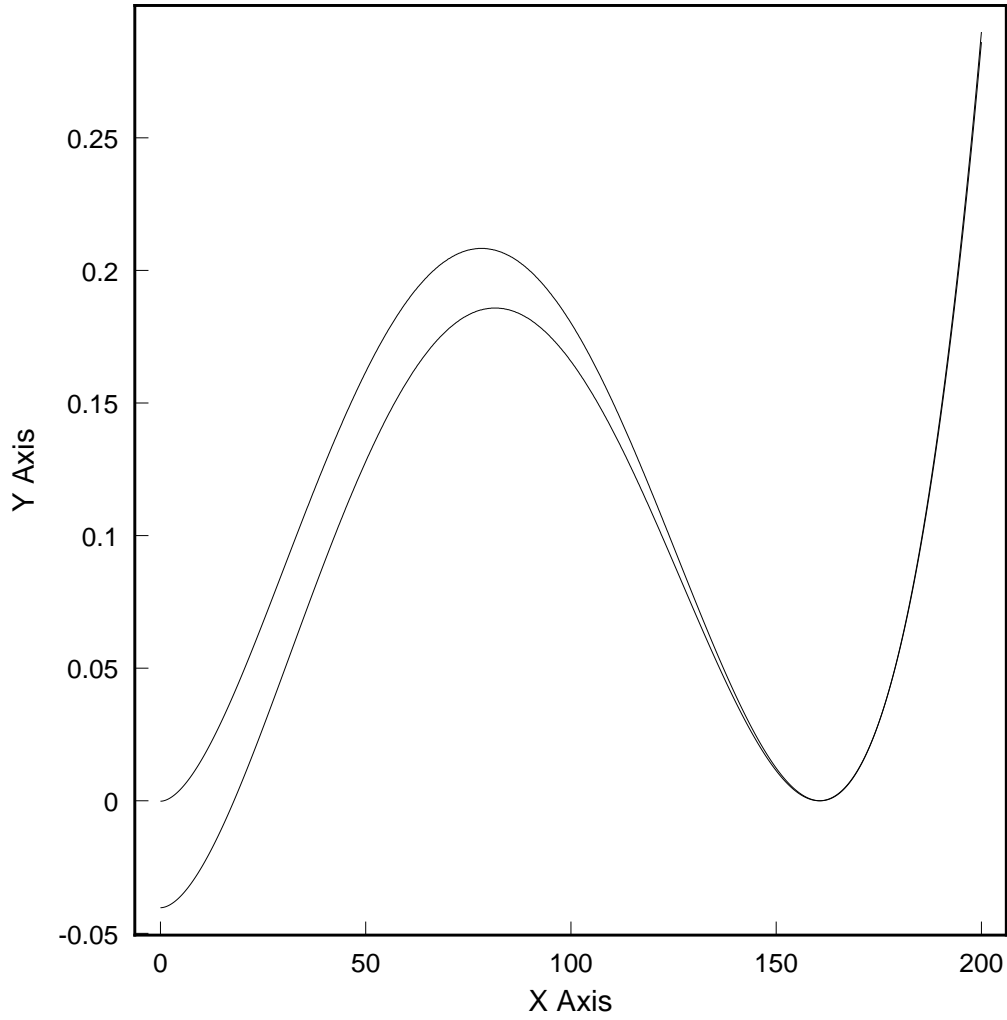


Figure 5: The two-loop (upper curve) and the one-loop (lower curve) rg improved effective potentials at the 2-loop critical temperature for $m_H = 35$ GeV. The x-axis is 4d scalar field, in GeV, the y axis is a dimensionless 3d potential $\frac{12}{g_3^6}V(\phi)$.

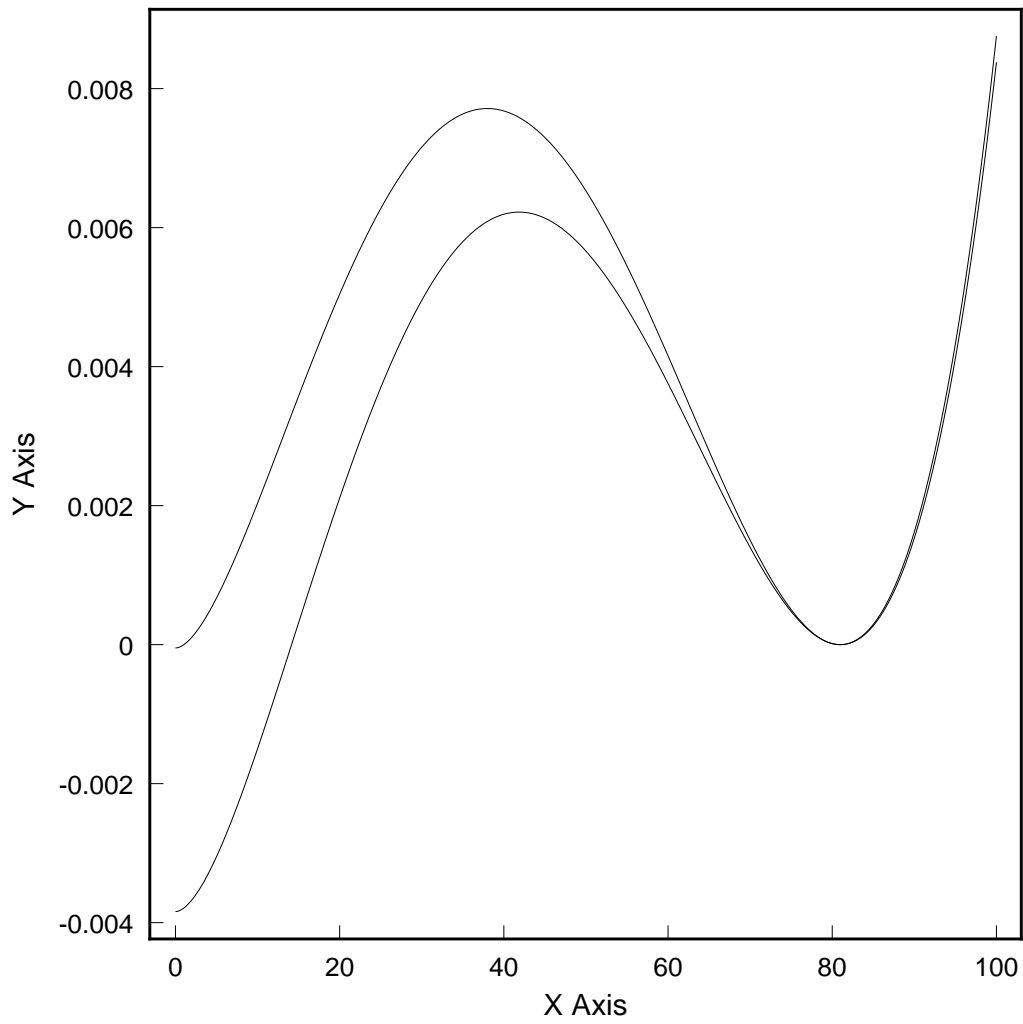


Figure 6: The same as in Fig. 5 for $m_H = 80\text{GeV}$.